DOI: 10.1002/chem.200700866

New and Efficient Arrays for Photoinduced Charge Separation Based on Perylene Bisimide and Corroles

Lucia Flamigni,*[a] Barbara Ventura,[a] Mariusz Tasior,[b] Thomas Becherer,[c] Heinz Langhals,*[c] and Daniel T. Gryko*[b]

Abstract: The bichromophoric systems **C2-PI**, **C3-PI**, and **C3-PPI** consisiting of corrole and perylene bisimide units and representing one of the rare cases of elaborate structures based on corrole, have been synthesized. Corroles **C2** and **C3** are, respectively, *meso*-substituted corroles with 2,6-dichlorophenyl and pentafluorophenyl substituents at the 5 and 15 positions. The three dyads were prepared by divergent strategy with the corrole-forming reaction as the last step of the sequence. **C2-PI** and **C3-PI** differ in the nature of the corroles, whereas **C3-PI** differs from **C3-PPI** in the presence of a further phenyl unit in the linker between photoactive units. The dyads display spectroscopic properties which are the superposition of the component spectra, indicating a very weak electronic coupling. Excitation of the corrole unit leads to charge separation with a rate which decreases from 2.4×10^{10}, to 5.0×10^{9}, and to $4.9\times10^{7}\ s^{-1}$ for **C2-PI**, **C3-PI**, and **C3-PPI**, respectively, where the reaction is characterized by a $\Delta G^{\circ}>0$. Excitation of the perylene bisimide unit is followed by competing reactions of: 1) energy transfer to the corrole unit, which subsequently deactivates to the charge-separated state and; 2) electron transfer to directly form the charge-separated state. The ratio of electron-to-energy-transfer rates is 9:1 and 1:1 for **C3-PI** and **C3-PPI**, respectively. The yield of charge separation is essentially 100% for **C2-PI** and **C3-PI**, and approximately 50% (excitation of peryleneimide) or 15% (excitation of the corrole) for **C3-PPI.** The lifetime of the charge-separated state, observed for the first time in corrole-based structures, is 540 ps for **C2-PI**, 2.5 ns for **C3-PI**, and 24 ns for **C3-PPI**, respectively. This is in agreement with an inverted behavior, according to Marcus theory.

Keywords: charge separation · corroles · electron transfer · photochemistry · porphyrinoids

Introduction

Light-induced processes and properties are receiving increasing interest regarding their potential use in several important fields. The search for new chromophores exhibiting photo- and electroactive properties which can complement or replicate the characteristics of already known dyes to be used in the construction of functional molecular arrays and materials is an important topic in synthetic and physical chemistry nowadays. In the last decades the efforts to increase the list of available chromophores adding new ones with specific absorption, emission, redox, and excited-state properties have produced a wide variety of compounds which can be usefully employed in the engineering of smart multicomponent structures able to perform light-driven actions.[1] The class of porphyrins has long been the most frequently used in the construction of these arrays[2] and has recently been extended with several new chromophores. Expanded porphyrins,[3] porphyrin tapes,[4] phthalocyanines,[5] subphthalocyanines,[6] chlorins,[7] porphyrins with an expanded π-conjugated system[8] have proven to be viable alternatives to simple porphyrins in the construction of photoactive dyads or higher homologues.

In this context, we have studied over the last few years the photophysical properties of free-base corroles and their potential use in the construction of assemblies with useful

[a] Dr. L. Flamigni, Dr. B. Ventura
Istituto ISOF-CNR, Via P. Gobetti 101, 40129 Bologna (Italy)
Fax: (+39) 051-639-9844
E-mail: flamigni@isof.cnr.it

[b] M. Tasior, Dr. D. T. Gryko
Institute of Organic Chemistry of the Polish Academy of Sciences
Kasprzaka 44/52, 01–224 Warsaw (Poland)
Fax: (+48) 22-632-6681
E-mail: daniel@icho.edu.pl

[c] T. Becherer, Prof. Dr. H. Langhals
Department of Chemistry, LMU University of Munich
Butenandtstrasse 13, 81377 Munich (Germany)
Fax: (+49) 89-2180-77640
E-mail: Langhals@lrz.uni-muenchen.de

photoinduced properties. This research can be regarded as part of the more general and rapidly increasing interest in corroles, their synthesis, reactivity, and applications.[9] Concerning free base-corroles, we and others have shown that these tetrapyrrolic species, especially when bearing electron-withdrawing substituents, are photostable, display high luminescence, can sensitize singlet oxygen, have singlet and triplet excited states with well-characterized spectra and can be easily oxidized and reduced.[10,11,12] Free-base corroles can be connected to other units yielding photo- and thermally stable dyads able to undergo interesting photoinduced processes, such as energy[13,14,15] or electron transfer.[15] Herein we address the formation of charge-separated states following photoinduced electron transfer in new free-base corrole-based dyads. To have efficient electron transfer and the possibility to unambiguously identify and study the charge-separated states (CS) the corrole has been connected to a perylene bisimide unit. The latter is a stronger electron acceptor than the phenylene derivative and has similar electron affinity to the naphthalene bisimide ($E_{1/2}$ of the order of -0.5 V versus SCE). It also has a well-characterized and extremely intense spectrum of the reduced radical ($\varepsilon \approx 100\,000\,\text{M}^{-1}\,\text{cm}^{-1}$) in the near-infrared (NIR) spectral region and therefore is very useful in the characterization and study of the CS state.[16–18]

Results and Discussion

Design and synthesis: Several issues merit particular consideration when contemplating the synthesis of complex dyads that contain corrole. Regarding synthetic efficiency, in analogy to porphyrins, two general strategies are possible. The first starts with the synthesis of corrole followed by modifications of peripheral substituents. The second strategy starts with the preparation of an elaborated aldehyde which will then be used in the reaction that forms corrole. Given the moderate stability of corroles it is desirable to perform as few manipulations as possible. In this regard we decided to follow the second route as in our previous endeavor.[15] It is worth to mention that all dyads composed of perylene bisimide and porphyrin moieties studied to date (with one exception)[19] were synthesized by the opposite approach (that is, through joining both units).[7c,18i,19]

We decided to further build up our experience in the synthesis of *meso*-substituted *trans*-A_2B-corroles from dipyrromethanes and aldehydes.[20] This methodology allows the introduction of the desired substituent at the 10 position of the macrocycle core. The two remaining identical substituents at the positions 5 and 15 allow the control of other properties of the system, such as, solubility, stability, and redox properties. We envisaged the use of two different types of substituents at these positions: The strongly electron-withdrawing pentafluorophenyl group and the sterically hindered 2,6-dichlorophenyl group. This choice was induced by the desire to achieve reasonable stability and solubility of the dyads. As far as the linker connecting both chromophores is concerned we chose simple phenylmethylene and biphenylmethylene groups which should guarantee a good structural control and a sufficient electronic coupling to allow intramolecular processes.

In light of the considerations above, the crucial part of the synthesis of the dyads was the facile generation of the pivotal perylene bisimide core, endowed with an aldehyde functionality for further elaboration. Clearly, synthons for such synthesis need to possess both primary amino and formyl groups, but the formyl group needs to be present in a protected form. Additionally, the perylene bisimide unit has to show good solubility in common organic solvents,[21] possess a formyl group, and be robust. A few different approaches have been proposed towards producing perylene bisimides with good solubility. The most common is to use 2,6-diisopropylphenylamine[19] or 2,5-di-*tert*-butylphenylamine[22] as solubilizing moieties. After preliminary experiments we decided to focus on less common, but more efficient "swallow-tail" aliphatic amines introduced by Langhals.[23] We used monoimide-monoanhydride **4**[24] as the crucial building block which has to be combined with the unit containing free amino and protected aldehyde units. Suitable building block **3** was synthesized in two steps (Scheme 1) from 4-cyanobenzaldehyde (**1**).[25] Final condensation performed in melted imidazole[26] in the presence of zinc acetate afforded aldehyde **5** in 76% yield (Scheme 1). A chromatographic purification of initially formed acetal with silica[27] and ethanol proceeded with deprotection to form the aldehyde **5** directly. Although it is well described in the literature that mix-condensation of perylene bisanhydride (**6**) with two different amines leads almost exclusively to symmetrically substituted product,[21] we decided to try this approach as a conceptually simpler alternative pathway. Thus perylene-3,4,9,10-tetracarboxylic dianhydride **6**, amine **7**, and amine **8**[15] (bearing a masked formyl group) were heated in melted imidazole for 24 hours. After typical workup, we were delighted to find that all three possible products could be detected by using TLC. The column chromatography allowed us to separate the desired acetal from **PI0** and from the second symmetrical side product. Subsequent cleavage by using a DCM/TFA mixture afforded aldehyde **5** in 16% yield (after 2 steps).

The synthesis of aldehyde **14** bearing the elongated biphenylene unit took significantly longer although a similar method was used. The crucial biphenyl linkage was created through Suzuki coupling of 4-bromo-1-cyanobenzene (**9**) and 4-formylboronic acid (**10**) (Scheme 2).[28] The following protection with ethylene glycol and further reduction with LAH afforded amine **13** in 19% overall yield. Subsequent condensation with monoanhydride **4** afforded aldehyde **14** in 57% yield (Scheme 2). Both aldehydes were highly soluble in CH_2Cl_2 which is the typical solvent of choice in the synthesis of porphyrinoids.

Aldehydes **5** and **14** were subjected to conditions for the synthesis of *trans*-A_2B-corroles by using aldehydes and dipyrromethanes.[20] Poor solubility of perylene-aldehydes in MeOH precluded the use of otherwise superior H_2O/

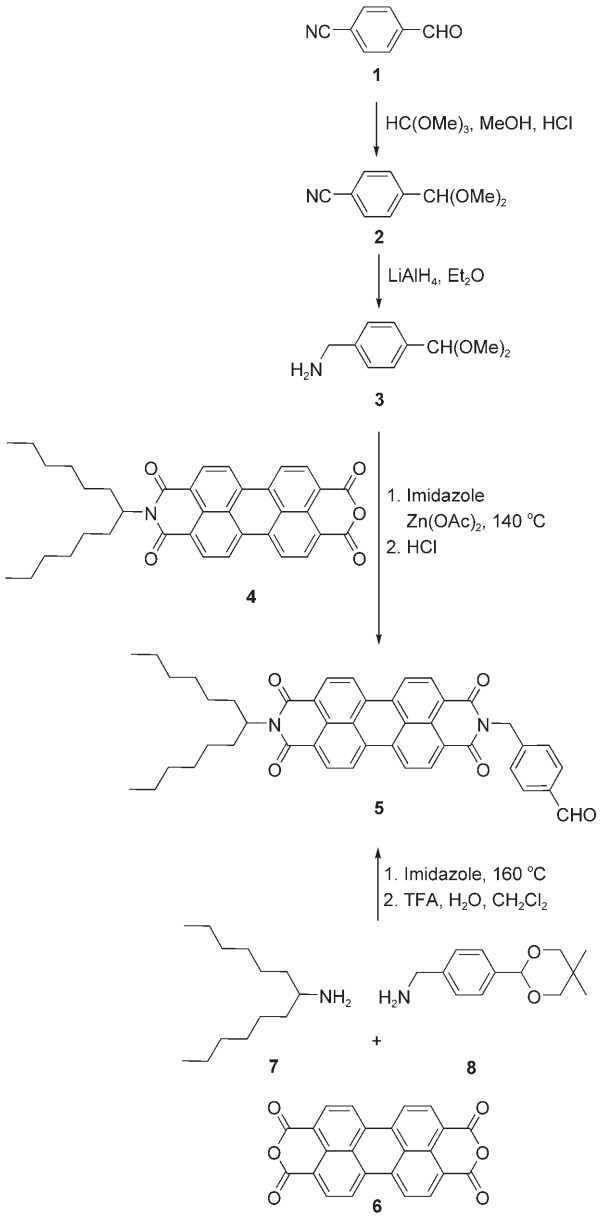

Scheme 1. The synthesis of aldehyde **5**.

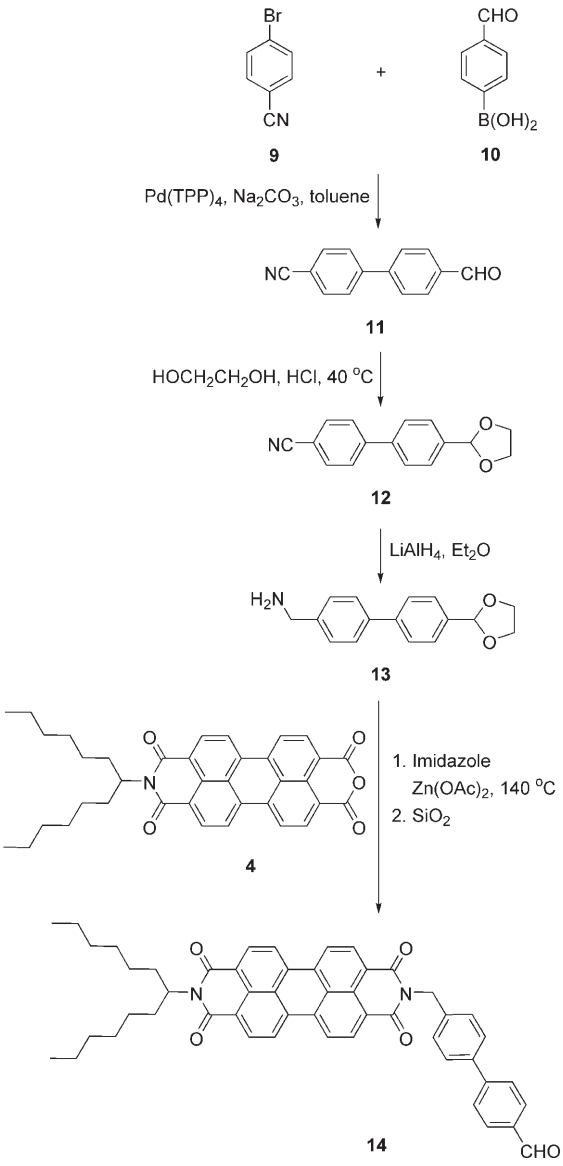

Scheme 2. The synthesis of aldehyde **14**.

MeOH/HCl conditions.[29] Consequently, we condensed dipyrromethanes **15** and **16** with aldehyde **5** in CH_2Cl_2 in the presence of TFA, under slightly more acidic conditions described in original publications.[20c,d] Quenching of the reaction with *p*-chloranil or DDQ resulted in the corresponding dyads **C2-PI** and **C3-PI** in 14 and 15% yields, respectively (Scheme 3). Analogous condensation of aldehyde **14** with dipyrromethane **16** furnished dyad **C3-PPI** in 11% yield.

Photophysical properties

Absorption spectroscopy: A spectroscopic and photophysical investigation was carried out on corrole component models **C2**, **C3**, and on perylene bisimide model **PI0**, as well as, on the three dyads **C2-PI**, **C3-PI**, **C3-PPI**. The first two dyads have different substituents around the corrole periphery, 5,15-bis(2,6-dichlorophenyl)corrole moiety (**C2**), and a 5,15-bis(pentafluorophenyl)corrole moiety (**C3**) and the latter dyads have different distances between the perylene bisimide and the corrole component, having one or two phenyl groups, respectively, between the imidic nitrogen and the corrole *meso* position. The absorption spectra of the components superimposed with the spectrum of the dyad are reported in the three panels of Figure 1. Model **C2** displays a splitting of the Soret band previously discussed[15] and typical of corroles with a deviation from planarity of the macrocycle induced by crowding of substituents and reported for *meso* aryl groups bearing bulky *ortho* substituents.[12,11]

The dyads **C2-PI**, **C3-PI**, and **C3-PPI** display spectra which are essentially the superimposed absorption spectra of the component models, Figure 1. A very slight bathochro-

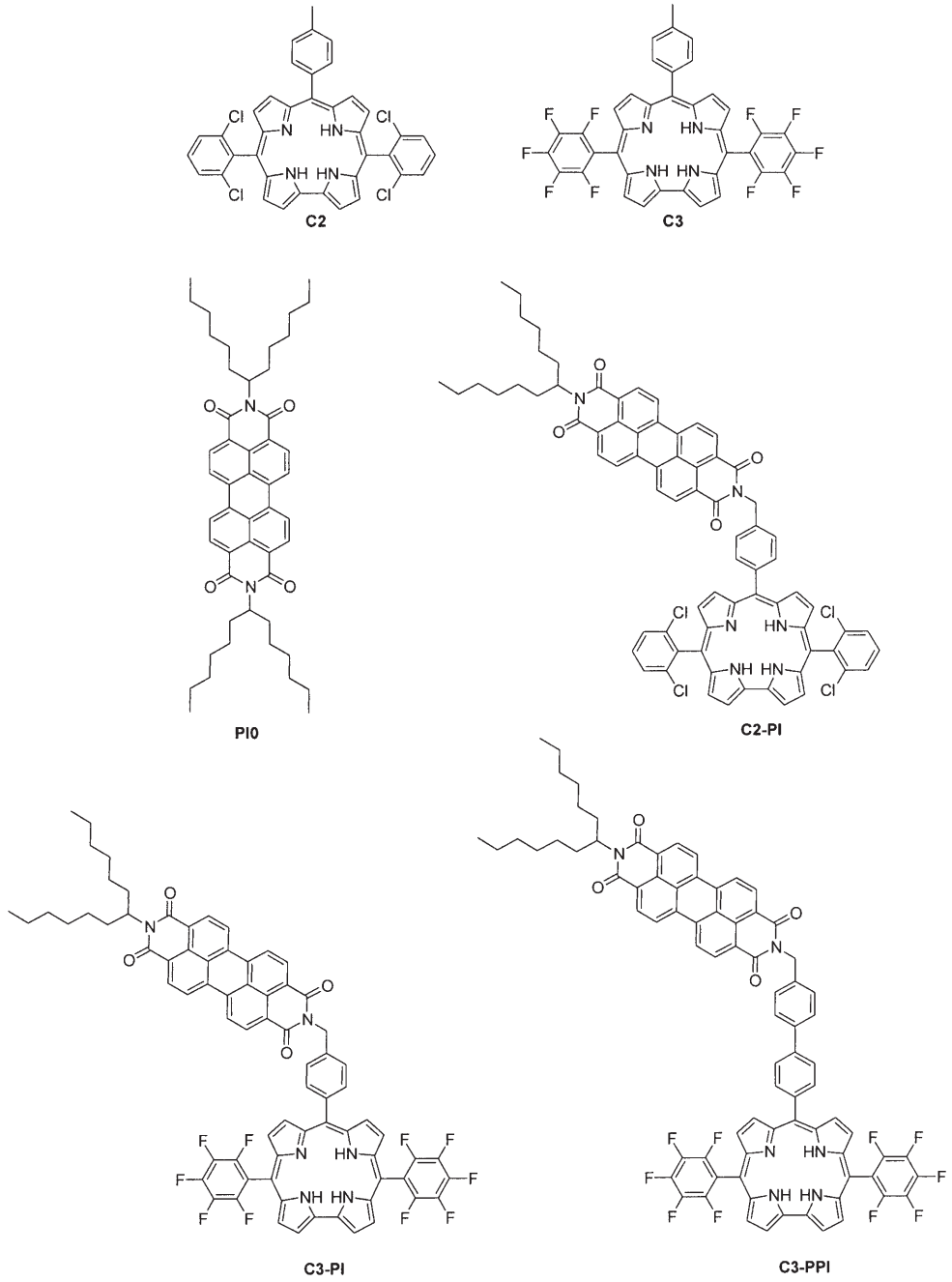

mic shift (2–3 nm) in the absorption maximum of the dyads with respect to the components can be noticed in **C2-PI** and **C3-PI**, but it is completely absent in **C3-PPI**, where the insertion of a further phenyl group electronically decouples components even more. In all cases, the good additive properties of the spectra indicate a very weak electronic coupling between the components and allow an approach based on a localized description of the individual subunits in the subsequent discussion of the photoinduced-energy and electron-transfer reactions.

From inspection of the spectra in Figure 1 one can see that selective excitation of the corrole component in the dyads is possible at wavelength >560 nm, whereas major excitation of the imide unit (about 85–90%) is possible on the two major peaks of the PI unit at 490 and 527 nm.

Luminescence spectroscopy: The luminescence spectra of model corroles **C2** and **C3** excited at 565 nm are reported in Figure 2. The luminescence spectra of the dyads **C2-PI**, **C3-PI, C3-PPI** selectively excited at the corrole units under the same experimental conditions are also shown in Figure 2. The fluorescence quantum yield of corroles is $\Phi_{fl}=0.06$ and 0.14 for **C2** and **C3**, respectively, whereas the fluorescence of the corrole units in the dyads decreases in a different

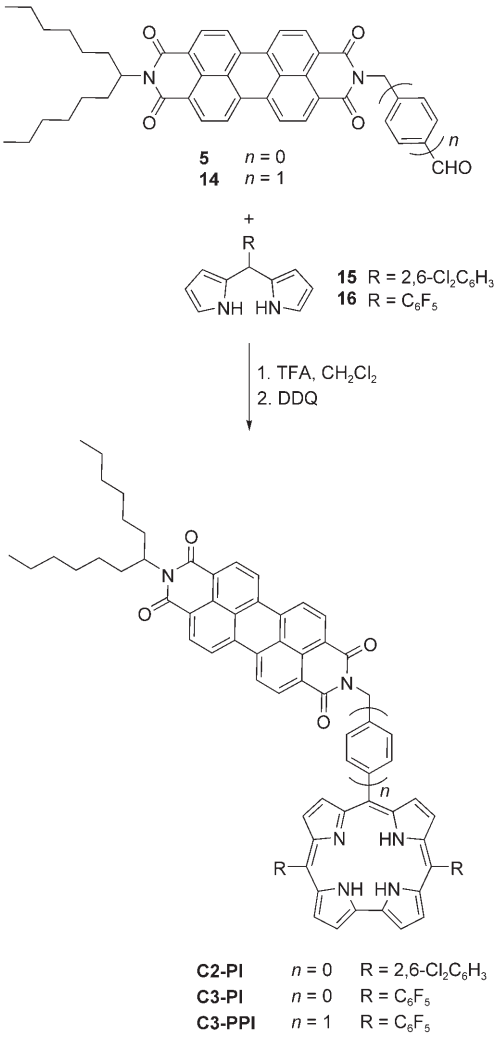

Scheme 3. The synthesis of dyads.

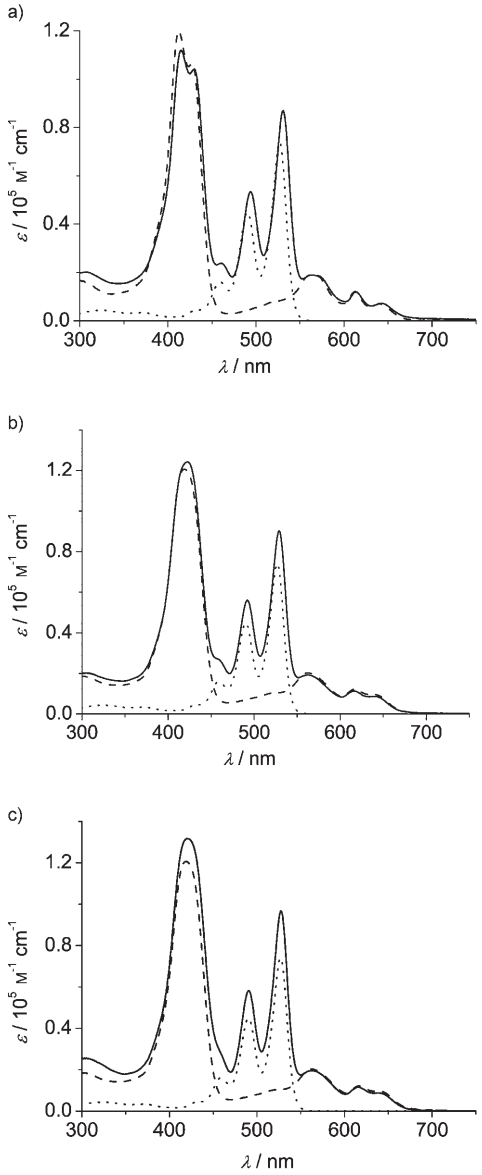

Figure 1. Absorbtion spectra of the model components and of the arrays in toluene. a) **C2** (– – –), **PI0** (••••), **C2-PI** (——); b) **C3** (– – –), **PI0** (••••), **C3-PI** (——); c) **C3** (– – –), **PI0** (••••), **C3-PPI** (——).

order: $\Phi_{fl} = 0.0015$, 0.0076, and 0.12 for **C2-PI**, **C3-PI**, and **C3-PPI**, respectively. The quenching is quite strong in the first two dyads, but it is only of the order of 15% in **C3-PPI**, characterized by a larger distance between bisimide and corrole. The results of excitation at 490 nm, where the PI unit is preferably excited (90% in **C2-PI**, 87% in **C3-PI** and **C3-PPI**, respectively), are shown in Figure 3. This compares the luminescence of the dyads with that of the models **PI0**, **C2**, or **C3** with concentrations adjusted to absorb the same number of photons as those absorbed by the pertinent unit in the dyad. The luminescence of **PI0** is scaled by a factor of 100 to better visualize the less intense emissions from the corroles and the dyads. The displayed results show that the emission of the perylene bisimide unit is quenched to less than 1% in all dyads, whereas the luminescence of corroles is quenched to 20 and 25% in **C2-PI** and **C3-PI**, respectively (less than upon selective excitation of the corrole unit), but it is increased by a factor of approximately four in **C3-PPI** (Figure 3). If one takes into account that at the excitation wavelength the absorbance of the corrole unit in **C3-PPI** is about 14% (see above) a quantitative sensitization of the corrole unit by the bisimide component would increase the corrole emission about seven times.

Time-resolved luminescence studies were performed by using a picosecond time-resolved system after excitation at 532 nm and a nanosecond-time-correlated single-photon counting apparatus following excitation at 560 nm (selective excitation of the corrole unit) and 465 nm (prevalent excitation of the bisimide unit). Models **C2**, **C3**, and **PI0** have lifetimes of 1.7, 3.8, and 4 ns, respectively, in toluene, at room temperature. Time-resolved spectra with picosecond resolution in the dyads **C2-PI**, **C3-PI**, and **C3-PPI** show the presence of the bisimide luminescence early on which decays during the pulse and leaves the luminescence of the corrole component. In all dyads the luminescence lifetime of the

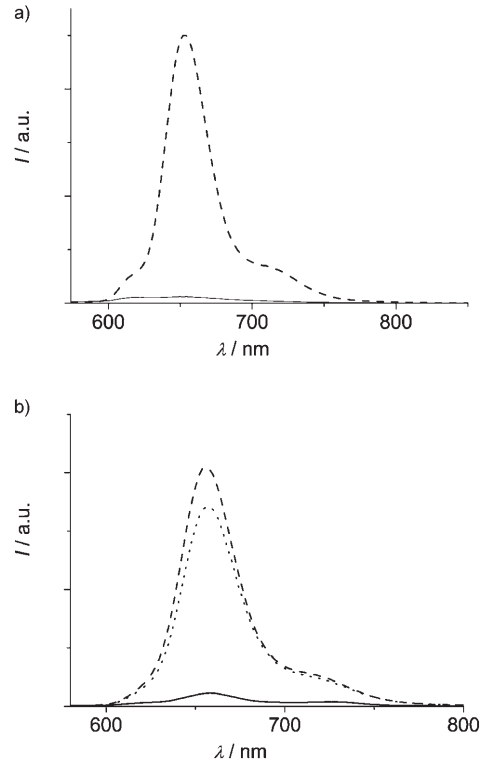

Figure 2. Room-temperature luminescence spectra in toluene of model corroles and dyads excited at 565 nm. a) **C2** (– – –) and **C2-PI** (——) $A=0.136$; b) **C3** (– – –), **C3-PI** (——), **C3-PPI** (•••••) $A=0.133$.

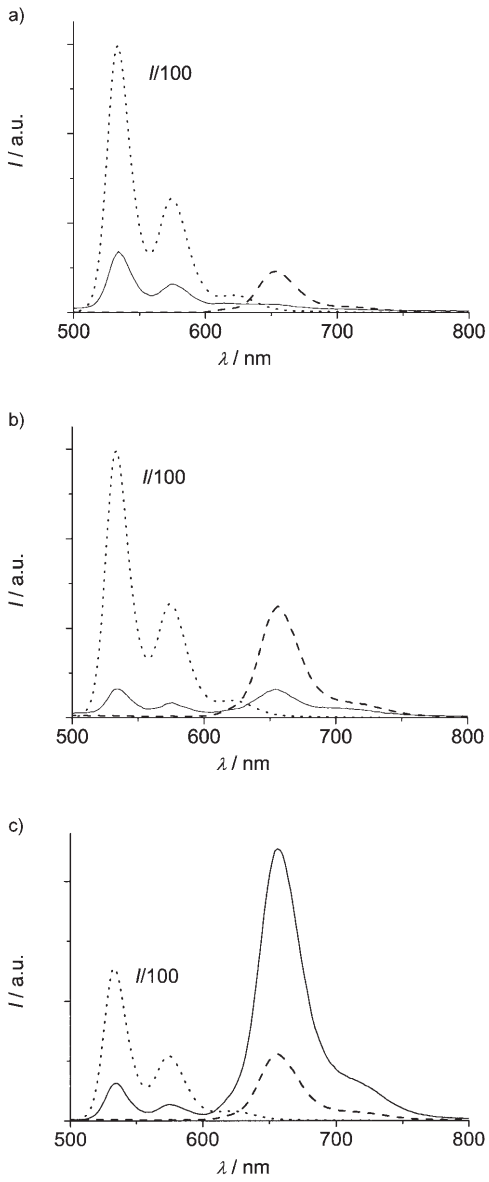

Figure 3. Room-temperature luminescence spectra in toluene of models and dyads excited at 490 nm. The luminescence of **PI0** is divided by 100. a) **C2** (– – –), **PI0** (•••••), **C2-PI** $A=0.12$ (——); b) **C3** (– – –), **PI0** (•••••), **C3-PI** $A=0.12$ (——); c) **C3** (– – –), **PI0** (•••••), **C3-PPI** $A=0.12$ (——). The absorbance of the solutions are arranged to provide the same numbers of photons absorbed by the reference model and the same unit in the arrays.

perylene bisimide unit is reduced to ≤ 10 ps (the time resolution of the apparatus). The lifetime of the corrole unit is decreased to 40 ps, 190 ps, and 3.2 ns in **C2-PI**, **C3-PI**, and **C3-PPI**, respectively (Figure 4). These values represent about 2, 5, and 85 %, respectively, of the lifetimes of the pertinent model, and are fully consistent with the reduction in luminescence quantum yield upon selective excitation of the corrole unit at 565 nm discussed above and amounting to 2.5, 5.4, and 86 % for **C2-PI**, **C3-PI**, and **C3-PPI**, respectively (Table 1). It is therefore clear that after excitation of the corrole unit in the dyad the excited state is depopulated by a process with an efficiency decreasing in the order **C2-PI** > **C3-PI** > **C3-PPI**, however, excitation of the bisimide under certain conditions causes an increase of the population of the excited state localized on corrole as verified by steady-state luminescence results. Time-resolved luminescence spectroscopy gives an "instant" picture rather than an "integrated" picture and indicates that the luminescent excited states of both imide and corrole undergo a decrease in lifetimes, in most cases very important. To obtain more insight on the mechanism of deactivation of the excited states, we determined the excitation spectra of the corrole luminescence at $\lambda=735$ nm. The spectra, reported in Figure 5, show that for all dyads excitation of perylene bisimide is effective (the typical absorption peaks of PI0 appear at 490 and 527 nm) in producing corrole luminescence although with different efficiencies, as the comparison with the normalized absorption spectra shows. This indicates the occurrence of an energy-transfer process from the bisimide excited state to the corrole, however the absence of quantitative sensitization of corrole luminescence in all dyads suggests the existence of other competitive processes which will be discussed below.

Luminescence spectra and lifetimes of the models were measured at 77 K in a glassy toluene matrix and are reported in Table 1 along with the room-temperature luminescence data. Model **PI0** shows the same lifetime as at room temperature, 4 ns, and a slight bathochromic shift. The corroles display a slight increase in the lifetime and nearly iden-

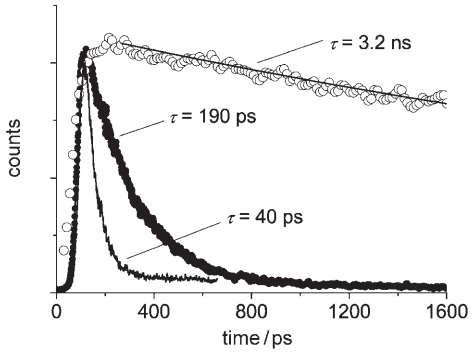

Figure 4. Time evolution of the luminescence registered at 650 nm from dyads in toluene after excitation with a laser pulse (35 ps, 532 nm, 1 mJ): **C2-PI** (——), **C3-PI** (●), and **C3-PPI** (○).

tical band maxima. Concerning the dyads, though a quantitative evaluation of emission quantum yields is prevented by geometric factors (see Experimental Section for emission at 77 K), some qualitative considerations can be derived. PI luminescence is nearly completely suppressed also at 77 K in all dyads; the luminescence of the corrole unit is not quenched or only slightly quenched in **C3-PI** and **C3-PPI**, but it is absent in **C2-PI** (data not shown).

Transient absorption spectroscopy: Valuable information on non-emitting intermediates formed during the deactivation process can be gained by transient absorption techniques. We performed transient absorbance experiments with picosecond resolution upon excitation at 532 nm. At this wavelength the perylene bisimide unit absorbs around 90% and the corroles about 10% of the photons.

The end-of-pulse transient absorption spectra detected with picosecond resolution of the models **C2**, **C3**, **PI0**, and the dyads **C2-PI** and **C3-PPI** are reported in Figure 6. The results for **C3-PI** show identical intensity and spectral shape to those for **C2-PI** and are not shown. The absorbances of the examined solutions have been arranged to provide the same absorbance of the model solutions as that of the corresponding unit in the array, in order to allow a direct comparison of the transient signals. Models **C2** and **C3** display absorption spectra attributed to the lowest singlet excited state ^{1}C2 or ^{1}C3 with negative features at 655 nm, due to the stimulated emission and positive absorbance above 750 nm.[10] The signal is, however, very weak under the experimental conditions. Model **PI0** displays negative signals around 575 and 625 nm, due to the lowest energy bands of the stimulated emission, and positive peaks at 690 and 855 nm,

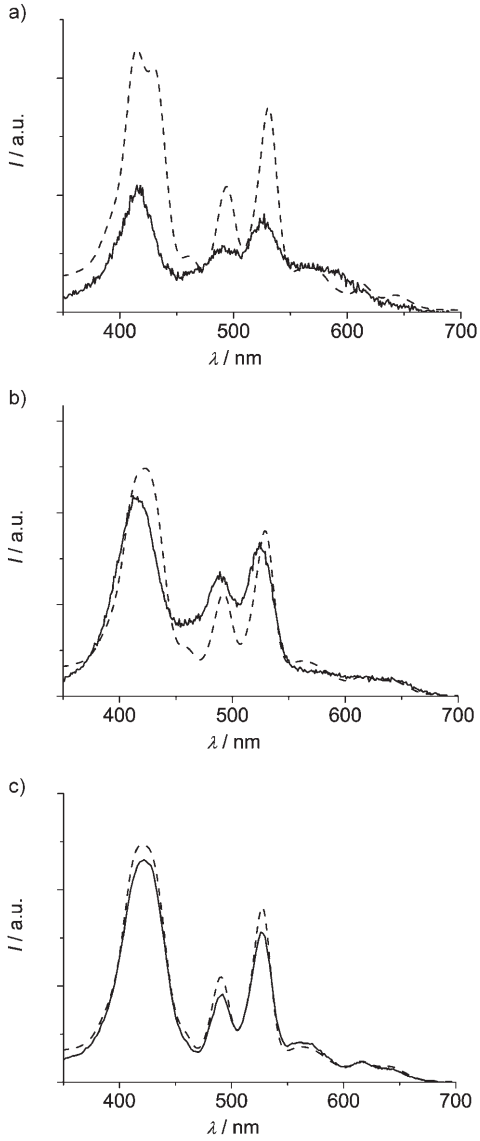

Figure 5. Excitation spectra measured at 735 nm (——) and absorption spectra normalized in the corrole Q-band region (– – –). a) **C2-PI**; b) **C3-PI**; c) **C3-PPI**.

Table 1. Fluorescence data of dyads **C2-PI, C3-PI, C3-PPI**, and models in air-equilibrated toluene at 295 K, and in rigid toluene glass at 77 K.

		295 K					77 K		
	State	λ_{max} [nm]	Φ_{fl}[a]	Φ_{fl}[b]	Φ_{fl}[c]	τ [ns][d]	λ_{max} [nm]	τ [ns][d]	E [eV][e]
PI0	^{1}PI0	534, 574, 622	0.92			4.0	543, 587, 638	4.0	2.28
C2	^{1}C2	653, 710 (sh)	0.06			1.7	652, 717	2.5	1.90
C2-PI	C2-^{1}PI	535, 576			0.0021	$\leq$10 ps	543, 587		2.28
	^{1}C2-PI	652		0.0015	0.013	40 ps	653		1.90
C3	^{1}C3	656, 716 (sh)	0.14			3.8	654, 718	5.2	1.90
C3-PI	C3-^{1}PI	535, 575			0.0010	$\leq$10 ps	543, 587		2.28
	^{1}C3-PI	658, 728 (sh)		0.0076	0.036	190 ps	654, 720		1.90
C3-PPI	C3-^{1}PPI	534, 574			0.0023	$\leq$10 ps	543, 585		2.28
	^{1}C3-PPI	657, 720 (sh)		0.12	0.54	3.2	656, 718	5.0	1.89

[a] Luminescence yields in air-equilibrated solutions, excitation at 490 nm for **PI0** and at 560 nm for corroles. [b] Luminescence yields upon selective excitation of corrole component at 565 nm. [c] Luminescence yields upon excitation at 490 nm, absorption of the PI component in the dyads is about 90%. [d] Excitation at 465, 560, and 532 nm for **PI0**, corroles, and dyads, respectively. [e] Derived from the emission maxima at 77 K.

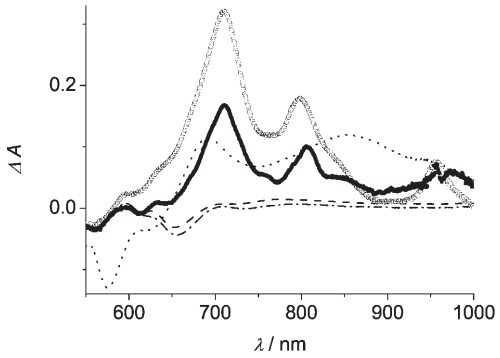

Figure 6. End-of-pulse absorption spectra of **C2** (– – –) $A=0.05$, **C3** (–•–•) $A=0.05$, **PI0** (•••••) $A=0.43$, **C3-PI** $A=0.6$ (○), **C3-PPI** $A=0.6$ (●), **C2-PI** $A=0.6$ is superimposable on that of **C3-PI** and not shown. The absorbance of the solutions has been adjusted to provide the same light absorbance by the unit in the model and in the dyad.

assigned to the singlet excited state ^{1}PI0. The decay of the spectra in the time window of the experiment (0–3.3 ns) is low, but compatible with a lifetime of 4 ns, confirming the assignment to the lowest singlet excited state. The spectra in the dyads are characterized by very strong features with maxima at 710, 800, and 960 nm identical for the three dyads, but in **C3-PPI** the intensity of the signal is only half that in **C2-PI** and **C3-PI**. Since these bands are not present in the component units and they appear very quickly, we have to assign them to the product of an intramolecular process. According to previous spectroelectrochemical characterization, they can be assigned to the perylene bisimide anion.[16,17] To explain this, we assume that intramolecular transfer of an electron takes place leading to the formation of a charge-separated state (CS) with the hole localized on the corrole unit and the electron on the PI unit.[18] The time evolution of the bands assigned to CS is different for the different dyads. In Figure 7 the time-resolved spectra taken at 710 nm with delays of 165 ps for **C2-PI** and **C3-PI** are shown. The CS time evolution is characterized for both dyads by an immediate (during the laser pulse) formation and by a slower rise with lifetimes of 40 and 190 ps for **C2-PI** and **C3-PI**, respectively. This slower rise accounts for 20% of the total band intensity for **C3-PI** and for a value of the order of 30–50% for **C2-PI**, a more precise estimate is precluded by the timescale of the determination, which is close to the instrumental resolution. The formation is followed by an exponential decay to the baseline of the CS bands which is fitted by a single exponential with a lifetime of 540 ps for **C2-PI** and 2.5 ns for **C3-PI**. For **C3-PPI** the situation is different, there is essentially no decay of the CS bands in the time window explored by the picosecond experiment, about 3.5 ns, and a nanosecond flash-photolysis experiment was performed in order to detect the decay of the CS bands. Figure 8 shows the spectrum for air-purged solutions of **C3-PPI** in toluene at the end of the pulse and after the interfering emission signal coming from the perylene imide excited state. It displays the anion bands at 710 and 800 nm and decays exponentially with a lifetime of

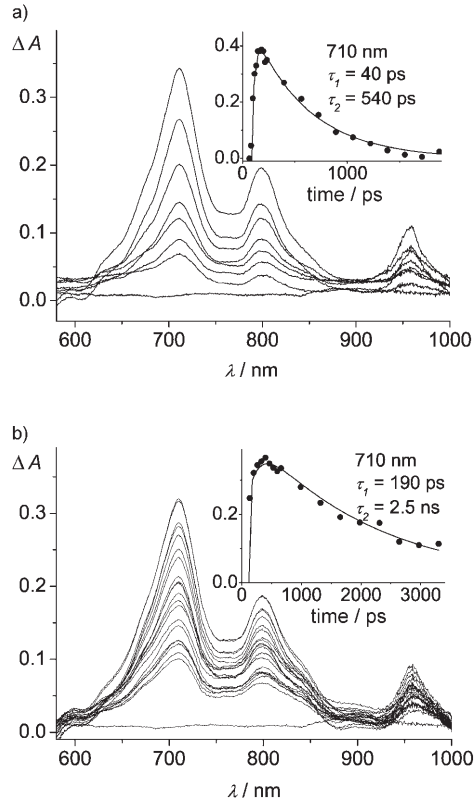

Figure 7. Time evolution of the transient spectra in toluene after excitation at 532 nm (3.3 mJ) taken with delays of 165 ps. In the insets, the time evolution of the absorbance at 710 nm and the biexponential fitting are shown. a) **C2-PI**, $A=0.6$; b) **C3-PI**, $A=0.6$.

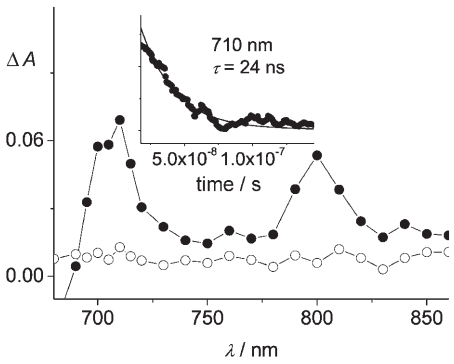

Figure 8. Time evolution of the transient spectrum of **C3-PPI** in toluene, $A=1.24$, after excitation with a nanosecond laser at 532 nm (3.5 mJ), spectra at 20 ns after the pulse (●) and at 120 ns after the pulse (○). In the inset, the time evolution of the absorbance at 710 nm and the exponential fitting are shown.

24 ns. The time resolution of this experiment, approximately 10 ns, did not allow the detection of the presence of a part that rises in the CS spectrum, similarly to what was detected for the other dyads **C2-PI** and **C3-PI**.

Photoinduced processes: To discuss the photoinduced processes occurring in the dyads it is convenient to introduce

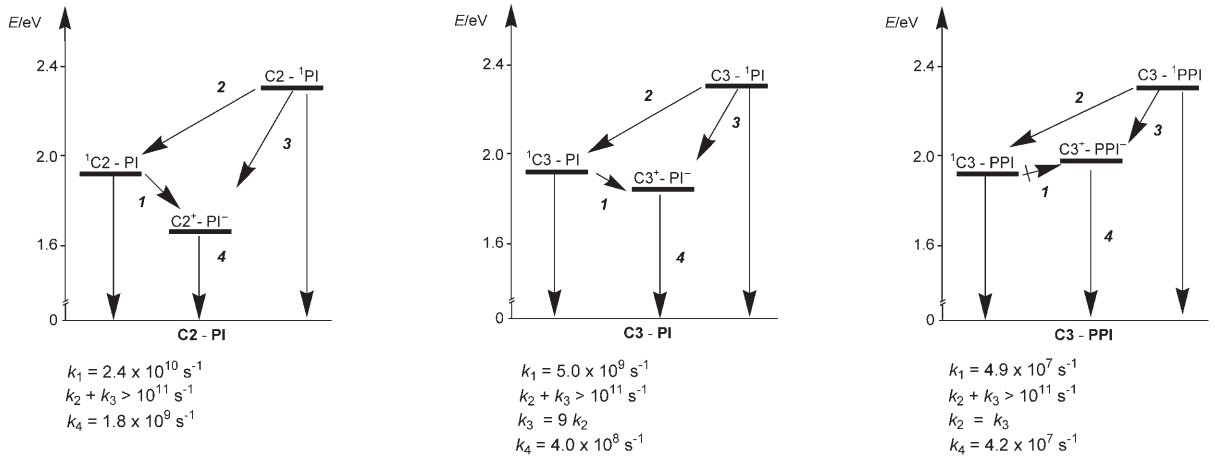

Scheme 4. Energy level diagrams and main reaction paths following excitation of **C2-PI**, **C3-PI**, and **C3-PPI**.

the energy level diagram showing the energy of the excited states and of the states originating from possible intramolecular reactions, such as the CS derived from the transfer of an electron from one component to the other (Scheme 4). The excited-state energy levels are derived from the luminescence maxima at 77 K shown in Table 1 and the CS energy levels are derived from the energy necessary to reduce the acceptor and oxidize the donor after correction for the different solvents used in the photophysical experiments and in the electrochemical determinations. Electrochemical data are available from the literature, the phenyl-substituted compound corresponding to **PI0** reduces at -0.92 V versus Fc^+/Fc in acetonitrile[16] which is converted to -0.52 V versus SCE.[30]

Corroles are known to display irreversible oxidation at potentials which depend on the substitution pattern.[12] The one-electron oxidation is followed by fast chemical reactions which shift peak potentials to less positive values, thus oxidation peak potentials should be considered as lower limits of the thermodynamic oxidation potentials. For the present corroles, oxidation in benzonitrile occurs at $+0.72$ V versus SCE for **C2**, and at $+0.86$ V versus SCE for **C3**.[15] Given the very weak coupling of the components in the dyads (see spectroscopic data), we can reasonably assume that the above oxidation and reduction values are retained by the components in the dyads.

After corrections,[31,32] CS state levels in toluene are calculated at about 1.71, 1.85, and 1.96 eV for **C2-PI**, **C3-PI**, and **C3-PPI**, respectively; these figures should be considered as approximate values. It should be noticed that for all dyads the CS state involving the transfer of an electron from the bisimide to the corrole has higher energy than the excited states of the system, and will not be considered here.[33]

Selective excitation of the lowest singlet excited state of corrole units in the dyads, which was performed by using steady-state experiments at $\lambda = 565$ nm, indicates a very high quenching for the corrole luminescence except for **C3-PPI**, where quenching is only of the order of 15% (Table 1 and Figure 2). Time-resolved experiments agree with the steady-state luminescence data, see above. The only feasible process for quenching of the corrole unit is process ***1*** (see Scheme 4), electron transfer from excited corrole to the perylene bisimide to form the CS states $C2^+$-PI^-, $C3^+$-PI^-, and $C3^+$-PPI^-. However, whereas the $\Delta G°$ is positive ($\Delta G° = +0.07$ eV) for **C3-PPI**, it is slightly negative ($\Delta G° = -0.05$ eV) for **C3-PI**, and even more negative for **C2-PI** ($\Delta G° = -0.19$ eV). This allows a very fast reaction for **C2-PI** and a still efficient process in **C3-PI**, but a very slow reaction in **C3-PPI**, where the electron-transfer process is slowed down with respect to the similar **C3-PI** both by the unfavorable thermodynamics and by the increased distance between photoactive units. The reaction rates k_1 of this electron transfer can be calculated from the experimental lifetimes by the equation $k = 1/\tau - 1/\tau_0$, where τ and τ_0 represent the lifetimes of the excited state in the model and in the dyad, respectively (Table 1). The calculated rates are $k_1 = 2.4\times10^{10}$, 5×10^9, and 4.9×10^7 s^{-1} for **C2-PI**, **C3-PI**, and **C3-PPI**, respectively, unable in the latter to compete successfully with the intrinsic deactivation of corrole, $k = 1/\tau_0 = 2.6\times10^8$ s^{-1}.

When nearly selective excitation of the perylene bisimide unit at 490 nm is performed, a strong quenching of the ^{1}PI unit is detected, as well as a quenching of the corrole luminescence, except in the case of **C3-PPI**, where a sensitization of the luminescence of corrole is noted (Figure 3). This is indicative of an energy-transfer process from the PI unit to the corrole unit in the dyads, step ***2***, as confirmed by the excitation spectra, see Figure 5. Clearly the sensitized excited states ^{1}C2-PI, ^{1}C3-PI, and ^{1}C3-PPI undergo electron transfer as discussed above, resulting in a further strong quenching for the former two cases, whereas ^{1}C3-PPI which is only weakly quenched by electron transfer, appears sensitized. The luminescence lifetime of the PI unit in all dyads is reduced from 4 ns in the model to ≤ 10 ps, indicating a very efficient quenching, with a rate $\geq 10^{11}$ s^{-1}. The excited state localized on the perylene bisimide C2-^{1}PI, C3-^{1}PI, and C3-^{1}PPI can deactivate, in addition to step ***2***, through an electron transfer from ground-state corrole to yield the

charge-separated states C2$^+$-PI$^-$, C3$^+$-PI$^-$, and C3$^+$-PPI$^-$, step ***3*** (see Scheme 4). Both reactions are characterized by a strong driving force, $\Delta G° = -0.4$ eV for ***2*** and -0.57 eV $< \Delta G° < -0.32$ eV depending on the dyad, for process ***3***.

Charge separation can be produced both by step ***3*** and step ***1***, with different mechanisms. When the PI unit is excited, a reductive quenching of its excited state will occur, that is, the electron will move from the HOMO localized on the donor corrole to the HOMO localized on the perylene bisimide. When the corrole is excited, an electron will move from the LUMO localized on the donor to the LUMO on the perylene bisimide acceptor. Steps ***3*** and ***1*** can be distinguished by their kinetics; in the former case, the rate is very fast and formation occurs within the laser pulse whereas the latter process is characterized by slower rates coincident with the decay of corrole luminescence in the dyads, 2.4×10^{10}, 5×10^{9}, and 4.9×10^{7} s^{-1} for **C2-PI**, **C3-PI**, and **C3-PPI**, respectively. In agreement, two steps can be identified in the formation of the CS spectrum, as discussed in the section on transient absorbance, a fast step occurring during the pulse and a slower one with rates of 2.4×10^{10} and 5×10^{9} s^{-1} for **C2-PI** and **C3-PI**, respectively. For **C3-PPI** the timescale of the formation is too slow for the picosecond experiment and too fast for the nanosecond experiment and cannot be resolved (Figure 7). It should be noted that the CS spectrum ($\lambda_{max} = 710$, 800, and 960 nm) is essentially identical to that of the reduced perylene bisimide radical and no contribution can be detected from the corrole-oxidized radical. This is not surprising given the rather low molar absorption coefficient expected for the corrole cation, of the order of 10^4 similar to parent tetrapyrrole cations,[34] whereas the remarkably high molar absorption coefficient of the PI$^-$ radical, of the order of 100 000, can account for this observation.[16,17]

An estimate of the relative values of k_1 and k_2 can be attempted if one takes into account that the slower formation of CS ascribable to step ***1*** accounts for 20% of the total in **C3-PI** and that by excitation at 532 nm approximately 10% of the corrole excited state is formed directly by the absorption of light, a contribution of about 10% can be ascribed to sensitization of this state by the excited state of perylene bisimide (step ***2***). From this value an approximate estimate of the efficiency of the energy-transfer step ***2*** of about 10% can be derived for **C3-PI**, and $k_3 = 9k_2$ is calculated, indicating a minor contribution of energy-transfer step ***2*** with respect to electron-transfer step ***3***. A similar evaluation for **C2-PI** is difficult because of the uncertainty in the determination of the pre-exponential coefficient, see above.

Concerning the yield of the electron-transfer reaction, assuming a similar molar absorption coefficient for the CS of the different dyads, that is, C2$^+$-PI$^-$, C3$^+$-PI$^-$, and C3$^+$-PPI$^-$, CS yield in **C3-PPI** is about half that determined for the corresponding **C3-PI**. For the **C3-PI** a CS yield of about 100% can be assumed because nearly all photons eventually generate C3$^+$-PI$^-$ (see Scheme 4) and consequently for **C3-PPI** a CS yield of about 50% can be calculated. This is in good agreement with the sensitization of corrole luminescence by a factor of four detected in the steady-state experiment upon excitation at 490 nm, which corresponds to an efficiency of energy-transfer step ***2*** of around 50% (Figure 3). Therefore, for **C3-PPI**, k_3 is equal to k_2 which represents a noticeable increase of k_2 with respect to **C3-PI**, for which $k_3 = 9k_2$. This remarkable change in the relative value of the two rates seems to be due more to the change in the thermodynamic parameters of step ***3***, with a net decrease in driving force of the order of 0.11 eV from **C3-PI** to **C3-PPI**, rather than to the increase in distance between the donor and the acceptor, which would affect both energy- and electron-transfer rates. We will try to make a quantitative evaluation of such effects on each process below. Energy-transfer rates calculated according to a Förster mechanism are consistent with the experimental ones,[35,36] therefore, a dipole–dipole interaction mechanism is considered sufficient to explain the process, without requiring the contribution of an exchange mechanism (Dexter). However, the latter was found to be necessary to explain the high energy-transfer rates in several porphyrinic donor–acceptor systems connected by highly conjugated bridges.[37] With a Förster model we would expect a $1/R_{DA}^6$ dependence of the energy-transfer rate and consequently an increase in distance R from 13.5 Å for **C3-PI** to 17.7 Å for **C3-PPI** would lead to a fivefold reduction in k_2. Concerning the bridge-mediated electron transfer, it has recently been pointed out that the key parameter electronic coupling has a donor-bridge (and acceptor-bridge) energy gap dependence in addition to the most obvious donor–acceptor distance dependence.[38] This can cause a more complex formulation of electron-transfer rate than in terms of bridge type and length, that is, $k = A_0\exp(-\beta r_{DA})$ where β is considered a characteristic of the bridge. Though not accurate, for the present purposes the simpler exponential dependence with distance can be used with a damping factor $\beta = 0.4$ Å^{-1}, previously derived for electron-transfer processes between porphyrinic units connected by poly(phenylene) bridges.[39] Within this model, the increase in distance from **C3-PI** to **C3-PPI** would lead to an approximately fivefold decrease in rate, which is the same ratio found for the energy-transfer attenuation. Therefore, in the context of this simplified interpretation, a distance increase would affect both energy and electron transfer to the same extent and the reason for the decrease in electron-transfer efficiency from the excited state localized on PI seems to be ascribable to the change in thermodynamic parameters of the reactions. On the other hand the electron-transfer reaction from the excited state localized on corrole ^{1}C3-PPI, which has a positive $\Delta G°$, becomes very slow and noncompetitive with the intrinsic deactivation of the luminescence, in fact, the efficiency of electron transfer is only 15%.

Once CS has been formed through the steps discussed above, it recombines to the ground state without leaving any residual species, as verified by the absence of residual absorbance in the spectra. The recombination rates of the CS states are rather different and depend both on the thermodynamics of the process and on the distance of the reduced acceptor and oxidized donor which can favor a better cou-

pling and faster recombination. The lifetime of the CS state increases from 540 ps for a recombination $\Delta G°$ of about −1.71 eV in **C2-PI** to 2.5 ns for a $\Delta G°$ of about −1.85 eV in **C3-PI** and to a lifetime of 24 ns for a $\Delta G°$ of approximately −1.96 eV in **C3-PPI**; the reaction is very likely placed in the Marcus inverted region and, as such, its rate decreases by increasing the driving force.[40] In addition, for the latter two cases where a tenfold increase is registered, the parameter of the distance has, as discussed above, an important effect.

The lifetimes of charge-separated states in the system corrole/perylene bisimide are not very different from those reported for other tetrapyrrole/perylene bisimide dyads, ranging from hundreds of picoseconds to a few tens of nanoseconds (just one case reports a lifetime of one hundred picoseconds for a noncovalently linked array[5c]) depending on parameters like solvent, bond type, position of the connecting bridge, thermodynamics.[18a–k] However the 24 ns lifetime measured for the CS state in **C3-PPI** is one of the longest in covalently connected dyads, which is remarkable if one considers the relatively short center-to-center distance between the reacting units, less than 18 Å.

Conclusion

We proved that complex corrole dyads can be synthesized in an elegant way from respective perylene bisimide-aldehydes. Moreover it was shown that asymmetrically *N*-substituted perylene bisimides can be synthesized by mix-condensation in a moderate yield when the two employed amines display similar reactivity.

Upon illumination in an extended wavelength range (380–680 nm) the studied dyads can convert the light energy stored in their excited states into chemical energy, yielding charge-separated states with an electron localized on the perylene bisimide unit and a hole localized on the corrole component. The yield of charge separation changes from nearly 100% to about 50% for excitation of the perylene bisimide unit (100 and 15% for excitation of the corrole unit) and the lifetime of the charge-separated state varies from 0.54 to 24 ns. The relatively long lifetimes of the CS state compared to the close spacing of the counterparts (center-to-center distance of 13.5 Å for **C2-PI** or **C3-PI** and 17.7 Å for **C3-PPI**) render these arrays promising with respect to a possible utilization of the stored energy, eventually after further elaboration of the dyads into more complex structures. These systems represent important progress in photoactive multicomponent structures: 1) they contain a new, easily available tetrapyrrolic chromophore with good photochemical properties; 2) they have clearly overcome the previously reported instability of free-base corroles; 3) the properties reported here can favorably compare with those of the most frequently used porphyrin-based arrays, as shown by the lifetimes and yields of the CS states.

This confirms that free-base corroles are valuable components in the construction of artificial arrays for light energy conversion and open new possibilities for photovoltaic (light-to-electrical energy) and artificial photosynthetic (light-to-chemical energy) applications.

Experimental Section

Synthesis: All chemicals were used as received unless otherwise noted. Reagent-grade solvents (CH_2Cl_2, hexanes, cyclohexane) were distilled prior to use. All reported ^{1}H NMR and ^{13}C NMR spectra were recorded on Bruker AM 500 MHz or Varian 400 MHz spectrometer. Chemical shifts (δ [ppm]) were determined with TMS as the internal reference. UV/Vis spectra were recorded in toluene (Cary). Chromatography was performed on silica (silica gel 60, 200–400 mesh), or dry column vacuum chromatography (DCVC)[41] was performed on preparative thin-layer-chromatography silica (Merck 107747). Mass spectra were obtained by using EI, field desorption (FD) or electrospray MS (ESI-MS). The following compounds were synthesized according to the literature procedures: **4**,[24] **7**,[42] **8**,[15] **11**,[28] **15**,[43] **16**,[43] **PI0**,[44] **C2**,[15] and **C3**.[20d] The purity of all new corroles was established based on ^{1}H NMR spectra and elemental analysis.

4-(1,1-Dimethoxymethyl)benzonitrile (2): 4-Cyanobenzaldehyde (**1**, 4.85 g 37 mmol), trimethylorthoformiate (12.0 mL, 110 mmol), anhydrous methanol (150 mL), and 6 N HCl (7 drops) were heated at 40 °C for 3 h, stirred at room temperature for 12 h, treated with saturated aqueous Na_2CO_3 (10 mL), extracted three times with isohexane (20 mL each), dried ($MgSO_4$), evaporated in vacuo, and distilled in vacuo. Yield 5.09 g (78%) colorless liquid, b.p. 128–130 °C/18 mbar. Other physicochemical properties agree with published data.[25a]

4-(1,1-Dimethoxymethyl)benzylamine (4): 4-(1,1-Dimethoxymethyl)benzonitrile (**2**, 4.00 g, 22.6 mmol) in anhydrous diethyl ether (15 mL) was added dropwise to a suspension of lithium aluminum hydride (1.72 g, 45.2 mmol) in anhydrous diethyl ether (50 mL, 0 °C, Ar atmosphere) within 10 min, allowed to come to room temperature, stirred for 12 h, cooled (ice), treated dropwise with 20% aqueous NaOH with cooling (12 mL), and extracted three times with ether (50 mL each). The combined organic phases were dried ($MgSO_4$), filtered, and evaporated in vacuo. Yield 2.37 g (58%) yellowish oil, $n_D^{20}=1.528$; ^{1}H NMR (300 MHz, $CDCl_3$, 25 °C): $\delta=1.55$ (s, 2H; NH_2), 3.31 (s, 6H; $2\times CH_3$), 3.86 (s, 2H; CH_2), 5.37 (s, 1H; CH), 7.30 (d, $^3J=8.2$ Hz, 2H; $CH_{arom.}$), 7.41 (d, $^3J=8.1$ Hz, 2H; $CH_{arom.}$); ^{13}C NMR (75 MHz, $CDCl_3$, 25 °C): $\delta=50.4$, 56.8, 107.3, 131.1, 140.9, 147.7 ppm; IR (ATR): $\tilde{\nu}=3375.9$ (w), 2989.8 (w), 2935.2 (m), 2828.6 (m), 1615.4 (w), 1511.7 (w), 1443.5 (w), 1414.7 (w), 1350.6 (m), 1303.1 (w), 1213.5 (m), 1191.8 (m), 1097.9 (s), 1047.1 (vs), 1019.6 (w), 979.7 (m), 908.8 (w), 806.1 (m), 770.6 (w), 658.2 cm^{-1} (w); MS (DEI$^+$/70 eV): *m*/*z* (%): 181 (5) [M^+], 150 (100) [M^+-CH_3O], 134 (17) [$M^+-C_2H_7O$], 120 (17) [$M^+-C_2H_5O_2$], 118 (24) [$M^+-C_2H_9NO$], 106 (6) [$M^+-C_3H_7O_2$], 91 (10) [$M^+-C_3H_8NO_2$], 77 (7) [$M^+-C_4H_{10}NO_2$], 75 (9) [$C_3H_7O_2$]; HRMS ($C_{10}H_{15}NO_2$): *m*/*z*: calcd: 181.110; found: 181.110; elemental analysis calcd (%) for $C_{10}H_{15}NO_2$ (181.2): C 66.30, H 8.34, N 7.73; found: C 66.42, H 8.54, N 7.82.

4-[9-(1-Hexylheptyl)-1,3,8,10-tetraoxo-3,8,9,10-tetrahydro-1*H*-anthra[2,1,9-*def*;6,5,10-*d′e′f′*]diisoquinoline-2-ylmethyl]benzaldehyde (5): *Method A*. 9-(1-Hexylheptyl)-2-benzopyrano[6′,5′,4′:10,5,6]anthra[2,1,9-*def*]isoquinoline-1,3,8,10-tetraone (**4**, 860 mg, 1.50 mmol), imidazole (17.0 g), and a microspatula quantity of zinc acetate ($Zn(OAc)_2\cdot 2H_2O$) were homogenized, heated under argon at 140 °C, treated with 4-(1,1-dimethoxymethyl)benzylamine (**3**, 460 mg, 2.55 mmol), heated at 140 °C for 2 h with stirring, allowed to cool, treated with ethanol (50 mL), precipitated with aqueous 2 M HCl (150 mL), collected by vacuum filtration, thoroughly washed with distilled water, dried in air at 110 °C for 16 h, and purified and deprotected with column separation (silica gel, chloroform/ethanol 40:1). Compound **5** was obtained after an orange-colored forerun as an intensely red-to-orange band and was dissolved in a small amount of chloroform and precipitated with acetonitrile. Yield 785 mg (76%). *Method B*. A dispersion of perylene-3,4,9,10-tetracarboxylic bisanhydride (**6,** 1.96 g, 5 mmol), 1-hexylheptylamine (**7,** 1.095 g, 6 mmol) and acetal **8** (1.215 g, 6 mmol) in imidazole (40 g) was heated at 160 °C,

for 24 h. The resulting mixture was diluted with water (20 mL) and 2 M HCl (140 mL) and allowed to sediment for 24 h. The precipitate was collected by vacuum filtration, washed with water, dried, and purified by column chromatography (silica, CH_2Cl_2, then CH_2Cl_2/acetone 98:2). The second fluorescent fraction was evaporated (mixture of acetal/aldehyde 9:1 based on NMR spectrscopy), the residue was dissolved in CH_2Cl_2/TFA/H_2O mixture (40:10:1, 51 mL), and stirred for 16 h. Saturated $NaHCO_3$ was carefully added and the organic phase was separated, washed with water, dried with Na_2SO_4, and evaporated. The pure aldehyde was obtained after refluxing with MeOH and filtration, red crystals, 540 mg, 16 % after 2 steps. M.p. = > 250 °C; R_f (silica gel, $CHCl_3$/EtOH 40:1) = 0.29; ^{1}H NMR (600 MHz, $CDCl_3$, 25 °C): δ = 0.82 (t, ^3J = 7.0 Hz, 6H; 2 × CH_3), 1.28 (m, 16H; CH_2), 1.87 (m, 2H; α-CH_2), 2.23 (m, 2H; α-CH_2), 5.18 (m, 1H; α-CH), 5.48 (s, 2H; NCH_2), 7.70 (d, ^3J = 8.2 Hz, 2H; $CH_{arom.}$), 7.85 (d, ^3J = 8.3 Hz, 2H; $CH_{arom.}$), 8.68 (m, 8H; $CH_{arom.}$), 9.98 ppm (s, 1H; CHO); ^{13}C NMR (125 MHz, $CDCl_3$): δ = 13.7, 22.3, 26.7, 28.9, 31.5, 32.1, 43.2, 54.6, 122.4, 122.5, 122.9, 126.0, 129.0, 129.1, 129.2, 129.7, 131.2, 134.6, 135.5, 143.5, 162.9, 191.5 ppm; IR (ATR): $\tilde{\nu}$ = 2953.8 (m), 2923.0 (s), 2855.3 (m), 1697.4 (s), 1646.4 (vs), 1610.0 (m), 1593.4 (s), 1577.3 (m), 1506.9 (w), 1436.2 (m), 1403.9 (m), 1378.2 (w), 1336.1 (s), 1301.7 (w), 1249.8 (m), 1212.4 (w), 1199.7 (w), 1168.2 (m), 1125.2 (w), 1106.0 (w), 987.0 (w), 849.6 (w), 823.9 (w), 808.9 (m), 774.3 (w), 742.6 (m), 723.1 (w), 631.4 cm^{-1} (w); UV/Vis ($CHCl_3$): λ_{max} (ε) = 459.1 (18600), 491.0 (51400), 527.4 nm (85800); fluorescence ($CHCl_3$): λ_{max} (I) = 534.5 (1.00), 578.0 nm (0.50), fluorescence quantum yield ($CHCl_3$, λ_{exc} = 491 nm, $E_{491\,nm}$ = 0.0212 cm^{-1}, reference: 2,9-bis-(1-hexylheptyl)anthra[2,1,9-*def*;6,5,10-*d′e′f′*]diisoquinoline-1,3,8,10-tetraone with Φ = 1.00): 1.00; MS (DEI$^+$/70 eV): m/z (%): 690 (33) [M^+], 508 (100) [$M^+ - C_{13}H_{26}$], 374 (14), [$M^+ - C_{21}H_{35}O_2$], 346 (19) [$M^+ - C_{22}H_{34}NO_2$], 44 (15) [CH_2NO]; HRMS: m/z: calcd: $C_{45}H_{42}N_2O_5$: 690.309; found: 690.308; elemental analysis calcd (%) for $C_{45}H_{42}N_2O_5$: C 78.24, H 6.13, N 4.06; found: C 77.98, H 6.01, N 4.05.

4′-(1,3-Dioxolan-2-yl)biphenyl-4-carbonitrile (12): 4′-Formylbiphenyl-4-carbonitrile (**11**, 1.45 g, 7.00 mmol) and ethylene glycol (1.74 g, 28.0 mmol) in toluene (50 mL) was allowed to react analogously to **2** and was crystallized from hexane/ethanol 5:1. Yield 610 mg (35 %) colorless crystalline solid, m.p. 170–171 °C; ^{1}H NMR (200 MHz, $CDCl_3$, 25 °C): δ = 4.02–4.21 (m, 4H; 2 × CH_2O), 5.87 (s, 1H; CH), 7.60–7.76 ppm (m, 8H; $CH_{arom.}$); ^{13}C NMR (150 MHz, $CDCl_3$, 25 °C): δ = 65.6, 103.5, 111.4, 119.1, 127.4, 127.5, 128.0, 132.8, 138.7, 140.3, 145.5 ppm; IR (ATR): $\tilde{\nu}$ = 3409.2 (w), 3070.0 (w), 2956.2 (m), 2884.5 (s), 2364.8 (w), 2225.5 (vs), 1930.0 (w), 1808.3 (w), 1699.7 (w), 1607.0 (s), 1555.9 (w), 1495.9 (m), 1481.2 (w), 1432.2 (m), 1401.8 (s), 1386.3 (s), 1312.4 (w), 1286.4 (w), 1227.2 (w), 1212.0 (w), 1184.5 (w), 1137.2 (w), 1117.2 (w), 1073.1 (s), 1021.8 (m), 1005.9 (w), 971.7 (m), 942.1 (m), 860.5 (w), 817.4 (vs), 720.2 (w), 689.9 (w), 648.7 cm^{-1} (w); MS (DEI+/70 eV): m/z (%): 251 (69) [M^+], 250 (100) [$M^+ - H$], 206 (35) [$M^+ - C_2H_5O$], 190 (21) [$M^+ - C_2H_5O_2$], 179 (72) [$M^+ - C_3H_4O_2$], 151 (17) [$M^+ - C_4H_6NO_2$], 73 (14) [$C_3H_5O_2$]; HRMS ($C_{16}H_{13}NO_2$): m/z: calcd: 251.095; found: 251.095.

4′-(1,3-Dioxolan-2-yl)biphenyl-4-methanamine (13): 4′-(1,3-Dioxolan-2-yl)-biphenyl-4-carbonitrile (**12**, 600 mg, 2.39 mmol) in THF (10 mL) and lithium aluminum hydride (181 mg, 4.78 mmol) in THF (10 mL) were allowed to react analogously to (1,1-dimethoxymethyl)benzylamine (**3**). Brown crystalline solid, yield 375 mg (62 %); m.p 120–123 °C; ^{1}H NMR (200 MHz, [D$_6$]DMSO, 25 °C): δ = 3.75 (s, 2H; CH_2), 3.92–4.12 (m, 4H; 2 × CH_2O), 5.77 (s, 1H; CH), 7.39–7.69 ppm (m, 8H; $CH_{arom.}$); ^{13}C NMR (100 MHz, [D$_6$]DMSO, 25 °C, TMS): δ = 45.9, 65.5, 103.3, 127.0, 127.1, 127.8, 128.3, 137.7, 138.4, 141.6, 144.2 ppm; IR (ATR): $\tilde{\nu}$ = 3380.3 (m), 3029.3 (w), 2953.7 (m), 2887.5 (s), 1915.2 (w), 1613.6 (w), 1562.6 (w), 1498.1 (m), 1432.5 (m), 1403.6 (m), 1382.7 (m), 1346.3 (w), 1310.3 (w), 1277.7 (w), 1205.8 (m), 1183.7 (w), 1114.2 (w), 1074.0 (vs), 1017.0 (m), 1003.6 (w), 964.8 (m), 939.1 (s), 877.8 (w), 838.2 (m), 798.0 (vs), 697.2 cm^{-1} (w); MS (DEI$^+$/70 eV): m/z (%): 255 (100) [M^+], 210 (14) [$M^+ - C_2H_5O$], 196 (6) [$M^+ - C_2H_3O_2$], 182 (42) [$M^+ - C_3H_5O_2$], 166 (40) [$M^+ - C_3H_7NO_2$], 152 (15) [$M^+ - C_4H_9NO_2$], 106 (18) [$M^+ - C_9H_9O_2$], 73 (25) [$C_3H_5O_2$]; HRMS ($C_{16}H_{17}NO_2$): m/z: calcd: 255.126; found: 255.126.

4′-[9-(1-Hexylheptyl)-1,3,8,10-tetraoxo-3,8,9,10-tetrahydro-1*H*-anthra[2,1,9-*def*;6,5,10-*d′e′f′*]diisoquinoline-2-ylmethyl]biphenyl-4-carbaldehyde (14): 9-(1-Hexylheptyl)-2-benzopyrano[6′,5′,4′:10,5,6]anthra[2,1,9-*def*]isoquinoline-1,3,8,10-tetraone (**4**, 400 mg, 0.697 mmol), 4′-(1,3-dioxolan-2-yl)biphenyl-4-methanamine (**13**, 350 mg, 1.37 mmol)), imidazole (10.0 g), and a microspatula quantity of zinc acetate ($Zn(OAc)_2 \cdot 2H_2O$) were allowed to react under argon as was described for **5** and the product was purified and deprotected by column separation (silica gel, chloroform/ethanol 40:1). The intensely reddish-orange main fraction was collected after an orange forerun and was evaporated, dissolved in the minimum amount of chloroform, and precipitated with acetonitrile. Bright light-red solid; yield 440 mg (57 %); m.p. > 250 °C, R_f (silica gel, $CHCl_3$/EtOH 40:1) = 0.28; ^{1}H NMR (600 MHz, $CDCl_3$, 25 °C, TMS): δ = 0.82 (t, ^3J(H;H) = 7.0 Hz, 6H; 2 × CH_3), 1.18–1.38 (m, 16H; 8 × CH_2), 1.83–1.91 (m, 2H; β-CH_2), 2.21–2.29 (m, 2H; β-CH_2), 5.15–5.22 (m, 1H; α-CH), 5.46 (s, 2H; NCH_2), 7.58–7.61 (m, 2H; CH_{aryl}), 7.67–7.72 (m, 4H; CH_{aryl}), 7.91–7.94 (m, 2H; CH_{aryl}), 8.59–8.71 (m, 8H; $CH_{perylene}$), 10.0 ppm (s, 1H; CHO); ^{13}C NMR (150 MHz, $CDCl_3$, 25 °C, TMS): δ = 14.3, 22.8, 27.2, 29.4, 32.0, 32.6, 43.7, 55.1, 123.2, 123.5, 126.6, 126.8, 127.7, 127.8, 129.7, 129.8, 129.9, 130.5, 132.0, 135.3, 135.4, 137.7, 139.3, 147.0, 163.7, 192.1 ppm; IR (ATR): $\tilde{\nu}$ = 2952.5 (m), 2924.0 (s), 2854.9 (m),1691.9 (s), 1650.2 (vs), 1592.6 (s), 1577.7 (m), 1506.5 (w), 1456.1 (w), 1434.7 (w), 1403.6 (m), 1378.0 (w), 1332.6 (s), 1247.0 (m), 1214.8 (w), 1169.3 (m), 1125.8 (w), 1106.2 (w), 1003.6 (w), 987.8 (w), 849.6 (w), 808.2 (m), 782.0 (w), 748.8 (w), 740.3 (w), 606.5 cm^{-1} (w); UV/Vis ($CHCl_3$): λ_{max} (ε $E_{rel.}$) = 459.2 (0.22), 490.4 (0.60), 527.0 nm (1.00); fluorescence ($CHCl_3$): λ_{max} ($I_{rel.}$) = 535.2 (1.00), 576.5 nm (0.50); fluorescence quantum yield ($CHCl_3$, λ_{exc} = 490 nm, $E_{490\,nm}$ = 0.0132 cm^{-1}, reference: 2,9-bis-(1-hexylheptyl)anthra[2,1,9-*def*;6,5,10-*d′e′f′*]diisoquinoline-1,3,8,10-tetraone with Φ = 1.00): 1.00; MS (DEI$^+$/70 eV): m/z (%): 766 (21) [M^+], 584 (100) [$M^+ - C_{13}H_{26}$], 346 (55) [$M^+ - C_{28}H_{38}NO_2$], 195 (14) [$C_{14}H_{11}O$]; HRMS ($C_{53}H_{50}N_2O_6$): m/z: calcd: 766.340; found: 766.339.

10-[(4-[9-(1-Hexylheptyl)-1,3,8,10-tetraoxo-3,8,9,10-tetrahydro-1*H*-anthra[2,1,9-*def*;6,5,10-*d′e′f′*]diisoquinoline-2-ylmethyl]phenyl)]-5,15-bis(2,6-dichlorophenyl)corrole (C2-PI): 2,6-Dichlorophenyldipyrromethane **15** (232 mg, 0.8 mmol) and aldehyde **5** (276 mg, 0.4 mmol) were dissolved in CH_2Cl_2 (6 mL). TFA (12 μL, 0.16 mmol) was added and mixture was stirred at RT for 20 min. Et_3N (22 μL, 0.16 mmol) was added followed by *p*-chloranil (296 mg, 1.2 mmol) and stirring was continued for 16 h. The reaction mixture was concentrated and was purified by chromatography (DCVC, silica, CH_2Cl_2). After evaporation, the residue was dissolved in THF and loaded on an SEC column (THF). The corrole fraction was collected, evaporated, refluxed with MeOH, and filtered to afford 70 mg (14 %) of corrole **C2-PI**. R_f = 0.5 (silica, CH_2Cl_2); ^{1}H NMR (500 MHz, $CDCl_3$) δ = −3–−1 (sbr, 3H; NH), 0.84 (t, J = 6.2 Hz, 6H; 2 × CH_3), 1.20–1.40 (m, 16H; alkyl), 1.85–1.95 (m, 2H; alkyl), 2.22–2.32 (m, 2H; alkyl), 5.15–5.25 (m, 1H; CH), 5.62 (s, 2H; CH_2), 7.60 (t, J = 8 Hz, 2H; $C_6H_3Cl_2$), 7.72 (d, J = 8 Hz, 4H; $C_6H_3Cl_2$), 8.09, 8.25 (AA′BB′, J = 6.5 Hz, 2 × 2H; C_6H_4), 8.28–8.70 (m, 14H; 8H; $C_{20}H_8$ + 6H; β-H), 8.97 ppm (d, J = 4 Hz, 2H; β-H); λ_{abs} (toluene, ε) = 413 (113), 428 (104), 459 (22.2), 492 (51.7), 528 (85.3), 561 (18.5), 611 (11.5), 640 nm (6.6 × 10^{-3}); ESI-LR obsd: 1246.3 [M^+ + H]; elemental analysis calcd (%) for $C_{75}H_{58}Cl_4N_6O_4$: C 72.12, H 4.68, N 6.73; found: C 72.24, H 4.87, N 6.58;

10-[(4-[9-(1-Hexylheptyl)-1,3,8,10-tetraoxo-3,8,9,10-tetrahydro-1*H*-anthra[2,1,9-*def*;6,5,10-*d′e′f′*]diisoquinoline-2-ylmethyl]phenyl)]-5,15-bis-(pentafluorophenyl)corrole (C3-PI): Pentafluorophenyldipyrromethane (**16**) (250 mg, 0.8 mmol) and aldehyde **5** (276 mg, 0.4 mmol) were dissolved in CH_2Cl_2 (6 mL). TFA (12 μL, 1.6 mmol) was added, and the mixture was stirred at room temperature. After 20 min Et_3N (22 μL, 0.16 mmol) was added followed by CH_2Cl_2 (14 mL). DDQ (590 mg, 2.6 mmol) was dissolved in toluene/CH_2Cl_2 (1:3, 20 mL) and both mixtures were added simultaneously to vigorously stirred CH_2Cl_2 (20 mL). After 15 min the reaction mixture was concentrated and was purified by chromatography (DCVC, silica, CH_2Cl_2). After evaporation, the residue was dissolved in THF and loaded on an SEC column (THF). The corrole fraction was collected, evaporated, refluxed with MeOH, and collected by vacuum filtration to afford 76 mg (15 %) of corrole **C3-PI**. R_f (silica, CH_2Cl_2) = 0.43; ^{1}H NMR (500 MHz, $CDCl_3$): δ = (−3)–(−1) (sbr, 3H; NH), 0.83 (t, J = 7 Hz, 6H; 2 × CH_3), 1.20–1.40 (m, 16H; alkyl), 1.85–1.95 (m, 2H; alkyl), 2.22–2.32 (m, 2H; alkyl), 5.10–5.20 (m, 1H; CH), 5.50 (sbr, 2H; CH_2), 8.09, 8.25 (AA′BB′, J = 6.5 Hz, 2 × 2H; C_6H_4), 8.28–8.70

(m, 14H; 8H; $C_{20}H_8$ and 6H; β-H), 8.93 ppm (d, $J=4$ Hz, 2H; β-H); λ_{abs} (toluene, ε) = 421 (124), 460 (25.5), 492 (57.7), 529 (94.4), 563 (19.6), 616 (11.6), 643 nm (8.8×10^{-3}); ESI-LR obsd 1290.5 [M^++H]; elemental analysis calcd (%) for $C_{75}H_{52}F_{10}N_6O_4\cdot H_2O$: C 68.98, H 4.27, N 6.35; found: C 68.95, H 4.08, N 6.48.

10-[4′-[9-(1-Hexylheptyl)-1,3,8,10-tetraoxo-3,8,9,10-tetrahydro-1*H*-anthra[2,1,9-*def*;6,5,10-*d′e′f′*]diisoquinoline-2-ylmethyl]biphenyl-4-]-5,15-bis(pentafluorophenyl)corrole (C3-PPI): Pentafluorophenyldipyrromethane (**16**) (125 mg, 0.4 mmol) and aldehyde **14** (153 mg, 0.2 mmol) were dissolved in CH_2Cl_2 (6 mL). TFA (6 μL, 0.8 mmol) was added, and the mixture was stirred at room temperature. After 40 min, Et_3N (44 μL, 0.16 mmol) was added, followed by CH_2Cl_2 (306 mL). The reaction was quenched by addition of DDQ (118 mg, 0.52 mmol), dissolved in toluene (1 mL), and stirring was continued for 20 min. The reaction mixture was concentrated and was purified by chromatography (DCVC, silica, CH_2Cl_2). After evaporation, the residue was dissolved in THF and loaded onto an SEC column (THF). The corrole fraction was collected, evaporated, refluxed with MeOH, and filtered to afford 30 mg (11%) of corrole **C3-PPI**. $R_f=0.6$ (silica, CH_2Cl_2); ^{1}H NMR (500 MHz, $CDCl_3$): δ = (−3)–(−1) (sbr, 3H; NH), 0.84 (t, $J=7$ Hz, 6H; $2\times CH_3$), 1.20–1.40 (m, 16H; alkyl), 1.86–1.96 (m, 2H; alkyl), 2.22–2.32 (m, 2H; alkyl), 5.15–5.25 (m, 1H; CH), 5.34 (sbr, 2H; CH_2), 7.72, 8.86 (AA′BB′, $J=6.5$ Hz, $2\times$ 2H; C_6H_4), 7.90, 8.10 (AA′BB′, $J=6.5$ Hz, 2×2H; C_6H_4), 8.15–8.70 (m, 14H; 8H; $C_{20}H_8$ and 6H; β-H), 8.94 ppm (sbr, 2H; β-H); λ_{abs} (toluene, ε) = 422 (121), 491 (53.4), 528 (88.6), 564 (18.2), 617 (10.8), 643 nm (7.9×10^{-3}); FD-LR obsd. 1366.4 [$M^{\cdot+}$]; elemental analysis calcd (%) for $C_{81}H_{56}F_{10}N_6O_4$: C 71.15, H 4.13, N 6.15; found: C 71.02, H 3.88, N 5.96.

Spectroscopy and photophysics: Spectrophotometric grade toluene at 295 K and at 77 K was used without further purification. Standard 10-mm fluorescence cells were used at 295 K, whereas for experiments at 77 K, we used capillary tubes in a home-made quartz Dewar filled with liquid nitrogen. Due to these geometrical conditions at 77 K the absolute quantum yield could not be determined with confidence, only qualitative information could be derived. If not otherwise specified, solutions were air-equilibrated. Air-free solutions were bubbled for 10 min with a stream of argon in home-modified 10-mm fluorescence cells. A Perkin–Elmer Lambda 9 UV/Vis and a Spex Fluorolog II spectrofluorimeter were used to acquire absorption and emission spectra. Reported luminescence spectra were uncorrected unless otherwise specified. Emission quantum yields were determined after correction for the photomultiplier response, with reference to an air-equilibrated toluene solution of **PI0** in dichloromethane with a $\Phi_{fl}=0.99$,[45] or to TPP with a $\Phi_{fl}=0.11$,[46] for corroles. Luminescence lifetimes in the nanosecond range were obtained with an IBH single-photon counting apparatus with excitation at 465 or 560 nm from pulsed-diode sources (resolution 0.3 ns). For determination of emission lifetimes in the picosecond range an apparatus based on a Nd:YAG laser (35 ps pulse duration, 532 nm, 1.5 mJ) and a Streak Camera with overall resolution of 10 ps was used.[47] Transient absorbance in the picosecond range made use of a pump and probe system based on a Nd:YAG laser (Continuum PY62/10, 35 ps pulse). The second harmonic (532 nm) at a frequency of 10 Hz and an energy of about 3.5 mJ/pulse was used to excite the samples the absorbance of which at the excitation wavelength was approximately 0.6. The residual 1064 nm light (about 40 mJ) was focused on a stirred 10-cm cell containing a mixture of D_2O/D_3PO_4 to produce a white-light continuum which was used as analyzing light. A computer-controlled optical delay stage (Ealing) on the path of the excitation beam provided a delay between excitation and analysis. The analyzing light was split in two parts probing irradiated and unirradiated portions of the sample, respectively, and crossed the sample cell in a nearly collinear geometry with respect to the excitation beam. The transmitted probes were fed through optical fibers into a spectrograph (Spectrapro 275, Acton) and were detected in two separate regions of a CCD detector (Princeton Instruments). The control units for the delay line, for the spectrograph and for the CCD detector were driven by customized software (Eurins) which also allowed spectral acquisition at increasing time delays between the pump and the probe. Typically, 200 to 500 laser shots were collected and averaged to obtain a single spectrum at a specific time delay. Kinetic analyses were made by selecting the absorbance values of successive time-resolved spectra at the selected wavelength and by applying standard iterative procedures. More details can be found elsewhere.[48] Nanosecond-laser flash-photolysis experiments were performed by using a system based on a Nd:YAG laser (JK Lasers, 532 nm, 3.5 mJ, 18 ns pulse) by using a right-angle analysis on the excited sample, previously described.[49]

Experimental uncertainties were estimated to be within 10% for lifetime determination, 15% for quantum yields, 20% for molar absorption coefficients, and 3 nm for emission and absorption peaks. The temperature of operation was 295 K except otherwise stated. Molecular dimensions were estimated after MM2 minimization by CS Chem3D Ultra 6.0 software.[50] Computation of the integral overlap and of the rate for the energy-transfer processes according to the Förster mechanism were performed with the use of Matlab 5.2.[51]

Acknowledgements

We thank CNR of Italy (PM.P04.010 MACOL), Ministero dell′Istruzione, dell′Università e della Ricerca of Italy (FIRB, RBNE019H9K), Polish Ministry of Research and Higher Education, the Deutsche Forschungsgemeinschaft and the Fonds der Chemischen Industrie for financial support.

[1] a) G. Kodis, Y. Terazono, P. A. Liddell, J. Andreasson, V. Garg, M. Hambourger, T. A. Moore, A. L. Moore, D. Gust, *J. Am. Chem. Soc.* **2006**, *128*, 1818–1827; b) E. H. A. Beckers, Z. Chen, S. C. J. Meskers, P. Jonkheijm, A. P. H. J. Schenning, X.-Q. Li, P. Osswald, F. Würthner, R. Janssen, *J. Phys. Chem. B* **2006**, *110*, 16967–16978; c) J. Segura, N. Martin, D. M. Guldi, *Chem. Soc. Rev.* **2005**, *34*, 31–47; d) S. Chakraborty, T. J. Wadas, H. Hester, R. Schmehl, R. Eisenberg, *Inorg. Chem.* **2005**, *44*, 6865–6878; e) M. H. Huynh, D. M. Dattelbaum, T. J. Meyer, *Coord. Chem. Rev.* **2005**, *249*, 457–483; f) L. Flamigni, E. Baranoff, J.-P. Collin, J.-P. Sauvage, *Chem. Eur. J.* **2006**, *12*, 6592–6606; g) M. Borgström, N. Shaikh, O. Johansson, M. F. Anderlund, S. Styring, B. Åkermark, A. Magnuson, L. Hammarström, *J. Am. Chem. Soc.* **2005**, *127*, 17504–17515; h) F. Giacalone, J. Segura, N. Martin, J. Ramey, D. M. Guldi, *Chem. Eur. J.* **2005**, *11*, 4819–4834; i) J. Daub, R. Engl, J. Kurzawa, S. E. Miller, S. Schneider, A. Stockmann, M. R. Wasielewski, *J. Phys. Chem. A* **2001**, *105*, 5655–5665; j) Y. Chen, M. E. El-Khouly, X.-D. Zhuang, N. He, Y. Araki, Y. Lin, O. Ito, *Chem. Eur. J.* **2007**, *13*, 1709–1714; k) R. Ziessel, G. Ulrich, A. Harriman, *New J. Chem.* **2007**, *31*, 496–501; l) M. R. Wasielewski, *J. Org. Chem.* **2006**, *71*, 5051–5066.

[2] a) D. Gust, T. A. Moore, A. L. Moore, *Acc. Chem. Res.* **2001**, *34*, 40–48; b) M. R. Wasielewski, *Chem. Rev.* **1992**, *92*, 435–461; c) L. Flamigni, V. Heitz, J.-P. Sauvage, *Struct. Bonding (Berlin)* **2006**, *121*, 217–261; d) K. Saito, Y. Kashiwagi, K. Ohkubo, S. Fukuzumi, *J. Porphyrins Phthalocyanines* **2006**, *10*, 1380–1391.

[3] Z. S. Yoon, J. H. Kwon, M.-C. Yoon, M. K. Koh, S. B. Noh, J. L. Sessler, J. T. Lee, D. Seidel, A. Aguilar, S. Shimizu, M. Suzuki, A. Osuka, D. Kim, *J. Am. Chem. Soc.* **2006**, *128*, 14128–14134.

[4] a) N. Mataga, S. Taniguchi, H. Chosrowjan, A. Osuka, N. Yoshida, *Photochem. Photobiol. Sci.* **2003**, *2*, 493–500; b) I. W. Hwang, T. Kamada, T. K. Ahn, D. M. Ko, T. Nakamura, A. Tsuda, A. Osuka, D. Kim, *J. Am. Chem. Soc.* **2004**, *126*, 16187–16198; c) K. Ogawa, Y. Kobuke, J. *Photochem. Photobiol. C* **2006**, *7*, 1–16; d) H. L. Anderson, *Chem. Commun.* **1999**, 2323–2330; e) T. V. Duncan, K. Susumu, L. E. Sinks, M. J. Therien, *J. Am. Chem. Soc.* **2006**, *128*, 9000–9001.

[5] a) X. Li, L. E. Sinks, B. Rybtchinski, M. R. Wasielewski, *J. Am. Chem. Soc.* **2004**, *126*, 10810–10811; b) D. M. Guldi, I. Zilbermann, A. Gouloumis, P. Vazquez, T. Torres, *J. Phys. Chem. B* **2004**, *108*, 18485–18494; c) M. S. Rodriguez-Morgade, T. Torres, C. Atienza-Castellanos, D. M. Guldi, *J. Am. Chem. Soc.* **2006**, *128*, 15145–15154.

[6] a) D. Gonzalez-Rodriguez, T. Torres, D. M. Guldi, J. Rivera, M. A. Herranz, L. Echegoyen, *J. Am. Chem. Soc.* **2004**, *126*, 6301–6313;

b) D. Gonzalez-Rodriguez, C. G. Claessens, T. Torres, S. G. Liu, L. Echegoyen, N. Vila, S. Nonell, *Chem. Eur. J.* **2005**, *11*, 3881–3893.
[7] a) V. Huber, M. Katterle, M. Lysetska, F. Würthner, *Angew. Chem. Int. Ed.* **2005**, *117*, 3208–3212; *Angew. Chem. Int. Ed.* **2005**, *44*, 3147–3151; b) S. Sasaki, T. Mizoguchi, H. Tamiaki, *Tetrahedron* **2005**, *61*, 8041–8048; c) R. F. Kelley, M. J. Tauber, M. R. Wasielewski, *J. Am. Chem. Soc.* **2006**, *128*, 4779–4791; d) C. Röger, M. G. Müller, M. Lysetska, Y. Miloslavina, A. R. Holzwarth, F. Würthner, *J. Am. Chem. Soc.* **2006**, *128*, 6542–6543; e) T. S. Balaban, *Acc. Chem. Res.* **2005**, *38*, 612–623.
[8] a) M. J. Crossley, P. J. Sintic, R. Walton, J. R. Reimers, *Org. Biomol. Chem.* **2003**, *1*, 2777–2787; b) L. Flamigni, M. R. Johnston, L. Giribabu, *Chem. Eur. J.* **2002**, *8*, 3938–3947.
[9] a) R. Paolesse in *The Porphyrin Handbook, Vol. 2* (Eds.: K. M. Kadish, K. M. Smith, R. Guilard), Academic Press, New York, **2000**, pp. 201–232; b) S. Nardis, D. Monti, R. Paolesse, *Mini-Rev. Org. Chem.* **2005**, *2*, 355–372; c) D. T. Gryko, J. P. Fox, D. P. Goldberg, *J. Porphyrins Phthalocyanines*, **2004**, *8*, 1091–1105; d) R. Guilard, J.-M. Barbe, C. Stern, K. M. Kadish in *The Porphyrin Handbook, Vol. 18* (Eds.: K. M. Kadish, K. M. Smith, R. Guilard), Elsevier Science, Boston, **2003**, pp. 303–349; e) Z. Gross, N. Galili, I. Saltsman, *Angew. Chem. Int. Ed.* **1999**, *111*, 1530–1533; *Angew. Chem. Int. Ed.* **1999**, *38*, 1427–1429; f) R. Paolesse, S. Nardis, F. Sagone, R. G. Khoury, *J. Org. Chem.* **2001**, *66*, 550–556; g) B. Ramdhanie, C. L. Stern, D. P. Goldberg, *J. Am. Chem. Soc.* **2001**, *123*, 9447–9448; h) J.-M. Barbe, G. Canard, S. Brandès, R. Guilard, *Angew. Chem.* **2005**, *117*, 3163–3166; *Angew. Chem. Int. Ed.* **2005**, *44*, 3103–3106; i) K. M. Kadish, J. Shao, Z. Ou, L. Frémond, R. Zhan, F. Burdet, J.-M. Barbe, C. P. Gros, R. Guilard, *Inorg. Chem.* **2005**, *44*, 6744–6754; j) R. Goldschmidt, I. Goldberg, Y. Balazs, Z. Gross, *J. Porphyrins Phthalocyanines* **2006**, *10*, 76–86; k) M. Bröring, F. Brégier, E. C. Tejero, C. Hell, M. C. Holthausen, *Angew. Chem.* **2007**, *119*, 449–452; *Angew. Chem. Int. Ed.* **2007**, *46*, 445–448; l) I. Aviv, Z. Gross, *Chem. Commun.* **2007**, 1987–1999; m) J. Poulin, C. Stern, R. Guilard, P. D. Harvey, *Photochem. Photobiol.* **2006**, *82*, 171–176; n) R. Paolesse, F. Sagone, A. Macagnano, T. Boschi, L. Prodi, M. Montalti, N. Zaccheroni, F. Bolletta, K. M. Smith, *J. Porphyrins Phthalocyanines* **1999**, *3*, 364–370; o) J. Sankar, H. Rath, V. Prabhuraja, S. Gokulnath, T. K. Chandrashekar, C. S. Purohit, S. Verma, *Chem. Eur. J.* **2007**, *13*, 105–114; p) R. Kumar, R. Misra, V. PrabhuRaja, T. K. Chandrashekar, *Chem. Eur. J.* **2005**, *11*, 5695–5707; q) S. Hiroto, K. Furukawa, H. Shinokubo, A. Osuka, *J. Am. Chem. Soc.* **2006**, *128*, 12380–12381; r) C. P. Gros, J.-M. Barbe, E. Espinoza, R. Guillard, *Angew. Chem.* **2006**, *118*, 5770–5773; *Angew. Chem. Int. Ed.* **2006**, *45*, 5642–5645; s) I. Aviv, Z. Gross, *Chem. Commun.* **2007**, 1987–1999.
[10] B. Ventura, A. Degli Esposti, B. Koszarna, D. T. Gryko, L. Flamigni, *New J. Chem.* **2005**, *29*, 1559–1566.
[11] a) T. Ding, E. A. Alemán, D. A. Mordarelli, C. J. Ziegler, *J. Phys. Chem. A* **2005**, *109*, 7411–7417; b) R. Paolesse, A. Marini, S. Nardis, A. Froiio, F. Mandoj, D. J. Nurco, L. Prodi, M. Montalti, K. M. Smith, *J. Porphyrins Phthalocyanines* **2003**, *7*, 25–36.
[12] J. Shen, J. Shao, Z. Ou, W. E. B. Koszarna, D. T. Gryko, K. M. Kadish, *Inorg. Chem.* **2006**, *45*, 2251–2265.
[13] L. Flamigni, B. Ventura, M. Tasior, D. T. Gryko, *Inorg. Chim. Acta* **2007**, *360*, 803–813.
[14] C. P. Gros, F. Brisach, A. Meristoudi, E. Espinosa, R. Guillard, P. D. Harvey, *Inorg. Chem.* **2007**, *46*, 125–135.
[15] M. Tasior, D. T. Gryko, M. Cembor, J. S. Jaworski, B. Ventura, L. Flamigni, *New J. Chem.* **2007**, *31*, 247–259.
[16] J. Salbeck, H. Kumkely, H. Langhals, R. W. Saalfrank, J. Daub, *Chimia* **1989**, *43*, 6–9.
[17] T. Kircher, H. G. Löhmannsröber, *Phys. Chem. Chem. Phys.* **1999**, *1*, 3987–3992.
[18] a) B. Rybtchinski, L. E. Sinks, M. R. Wasielewski, *J. Am. Chem. Soc.* **2004**, *126*, 12268–12269; b) L. Flamigni, B. Ventura, C.-C. You, C. Hippius, F. Würthner, *J. Phys. Chem. C* **2007**, *111*, 622–630; c) C. Flors, I. Oesterling, T. Schnitzler, E. Fron, G. Schweitzer, M. Sliwa, A. Herrmann, M. van der Auweraer, F. C. de Schryver, K. Mullen, J. Hofkens, *J. Phys. Chem. C* **2007**, *111*, 4861–4870; d) R. F. Kelley, W. S. Shin, B. Rybtchinski, L. E. Sinks, M. R. Wasielewski, *J. Am. Chem. Soc.* **2007**, *129*, 3173–3181; e) M. P. O'Neil, M. P. Niemczyk, W. A. Svec, D. Gosztola, G. L. Gaines III, M. R. Wasielewski, *Science* **1992**, *257*, 63–65; f) S. I. Yang, S. Prathapan, M. A. Miller, J. Seth, D. F. Bocian, J. S. Lindsey, D. Holten, *J. Phys. Chem. B* **2001**, *105*, 8249–8258; g) A. Prodi, C. Chiorboli, F. Scandola, E. Iengo, E. Alessio, R. Dobrawa, F. Würthner, *J. Am. Chem. Soc.* **2005**, *127*, 1454–1462; h) C. Kirmaier, E. Hindin, J. K. Schwartz, I. V. Sazanovich, J. R. Diers, K. Muthukumaran, M. Taniguchi, D. F. Bocian, J. S. Lindsey, D. Holten, *J. Phys. Chem. B* **2003**, *107*, 3443–3454; i) S. Prathapan, S. I. Yang, J. Seth, M. A. Miller, D. F. Bocian, D. Holten, J. S. Lindsey, *J. Phys. Chem. B* **2001**, *105*, 8237–8248; j) S. Xiao, M. E. El-Khouly, Y. Li, Z. Gan, H. Liu, L. Jiang, Y. Araki, O. Ito, D. Zhu, *J. Phys. Chem. B* **2005**, *109*, 3658–3667; k) M. J. Arhens, R. F. Kelley, Z. E. X. Dance, M. R. Wasielewski, *Phys. Chem. Chem. Phys.* **2007**, *9*, 1469–1478; l) W. E. Ford, H. Hiratsuka, P. V. Kamat, *J. Phys. Chem.* **1989**, *93*, 6692–6696; m) H. Langhals, U. Ritter, Persistent Perylene Bisimide Radical Anions as NIR Dyes, DE 102006011269.5, March 10, **2006**; n) H. Langhals, W. Jona, *Chem. Eur. J.* **1998**, *4*, 2110–2116; o) H. Langhals, S. Saulich, *Chem. Eur. J.* **2002**, *8*, 5630–5643.
[19] F. Graser, (BASF AG), DE 3049215, July 15, **1982**; [*Chem. Abstr.* **1982**, *97*, 129114].
[20] a) D. T. Gryko, K. Jadach, *J. Org. Chem.* **2001**, *66*, 4267–4275; b) D. T. Gryko, K. E. Piechota, *J. Porphyrins Phthalocyanines* **2002**, *6*, 81–97; c) D. T. Gryko, B. Koszarna, *Org. Biomol. Chem.* **2003**, *1*, 350–357; d) D. T. Gryko, B. Koszarna, *Synthesis* **2004**, 2205–2209;
[21] a) H. Langhals, *Helv. Chim. Acta* **2005**, *88*, 1309–1343; b) H. Langhals, *Heterocycles* **1995**, *40*, 477–500.
[22] a) H. Langhals, DE 3016764, April 30, **1980**; [*Chem. Abstr.* **1982**, *96*, P70417x]; b) H. Langhals, *Nachr. Chem. Tech. Lab.* **1980**, *28*, 716–718; [*Chem. Abstr.* **1981**, *95*, R9816q].
[23] a) S. Demmig, H. Langhals, *Chem. Ber.* **1988**, *121*, 225–230; b) H. Langhals, S. Demmig, T. Potrawa, *J. Prakt. Chem.* **1991**, *333*, 733–748.
[24] H. Kaiser, J. Lindner, H. Langhals, *Chem. Ber.* **1991**, *124*, 529–535.
[25] a) P. D. R. Rose, A. Williams, *J. Chem. Soc. Perkin Trans. 2* **2002**, 1589–1595; b) O. Ouari, F. Chalier, R. Bonaly, B. Pucci, P. Tordo, *J. Chem. Soc. Perkin Trans. 2* **1998**, 2299–2307.
[26] H. Langhals, *Chem. Ber.* **1985**, *118*, 4641–4645.
[27] The use of silica from Acros resulted in a complete deprotection whereas partial deprotection was observed with silica from Merck.
[28] M. A. Ismail, A. Batista-Parra, M. Adalgisa, Y. Miao, W. D. Wilson, T. Wenzler, R. Brun, D. W. Boykin, *Bioorg. Med. Chem.* **2005**, *13*, 6718–6726.
[29] B. Koszarna, D. T. Gryko, *J. Org. Chem.* **2006**, *71*, 3707–3717.
[30] N. G. Connelly, W. E. Geiger, *Chem. Rev.* **1996**, *96*, 877–910.
[31] A. Weller, *Z. Phys. Chem. (Muenchen Ger.)* **1982**, *133*, 93–98.
[32] The common correction used to determine the CS state energy level in an apolar solvent from the values of the redox potentials in a polar solvent takes into account the Coulombic interaction term and the ion solvation energy based on the Born dielectric continuum model according to Weller (ref. [31]). The energy of the charge-separated states relative to the ground state, ΔG_{CS}, can thus be calculated by the following equation: $\Delta G_{CS} = E_{ox} - E_{red} - (14.32/R_{DA}\varepsilon_S) + 14.32(1/2r_D + 1/2r_A)(1/\varepsilon_S - 1/\varepsilon_P)$ For the formation of the charge-separated state involving the transfer of an electron from the corrole to the perylene bisimide, E_{ox} and E_{red} are the first oxidation potential of the corrole and the first reduction potential of perylene bisimide, respectively, which are +0.72 V versus SCE for **C2**, +0.86 V versus SCE for **C3**, and −0.54 V versus SCE for **PI0**, $\varepsilon_S = 2.4$ is the dielectric constant of toluene, $\varepsilon_P = 31.2$ is an average of the dielectric constant of benzonitrile and acetonitrile. R_{DA}, the center-to-center donor–acceptor distance is 13.5 Å for **C2-PI** and **C3-PI**, and 17.7 Å for **C3-PPI**, and the perylene bisimide and corrole radii are taken $r_A = r_D = 6$ Å.
[33] The oxidation potential of **PI0** in acetonitrile is of the order of +1.6 V versus SCE and the reduction potential of corroles **C2** and

C3 are of the order of −0.75 V and −0.65 V versus SCE, respectively, in benzonitrile (M. Cembor, J. S. Jaworski, private communication), which would leave the CS energy level at about 1.7 eV after correction for the polarity of the solvent.

[34] J. Fajer, D. C. Borg, A. Forman, D. Dolphin, R. H. Felton, *J. Am. Chem. Soc.* **1970**, *92*, 3451–3459.

[35] Th. Förster, *Discuss. Faraday Soc.* **1959**, *27*, 7–17.

[36] The Förster rates k_{en}^{F} were calculated by means of Equation (1)[35]

$$k_{en}^{F}=\frac{8.8\times10^{-25}\kappa^{2}\Phi}{n^{4}\tau R_{DA}^{6}}J^{F} \quad (1)$$

in which Φ and τ are the emission quantum yield (0.92) and the lifetime (4 ns) of the donor PI, R_{DA} is the donor–acceptor center-to-center distance (13.5 Å for **C2-PI** and **C3-PI**, and 17.7 Å for **C3-PPI**), n is the refractive index of toluene and J^{F} is the overlap integral. κ^{2}, the orientation factor, can be simplified to the statistical value, 2/3. J^{F}, the Förster overlap integral, is calculated from the overlap between the luminescence spectrum of the donor **PI0**, $F(\tilde{\nu})$ (cm^{-1} units), and the absorption spectrum $\varepsilon(\tilde{\nu})$ of the acceptors **C2** and **C3** (cm^{-1} units), according to the Equation (2) (ref. [35])

$$J^{F}=\frac{\int F(\tilde{\nu})\varepsilon(\tilde{\nu})/\tilde{\nu}^{4}d\tilde{\nu}}{\int F(\tilde{\nu})d\tilde{\nu}} \quad (2)$$

From the experimental emission and absorption spectra an overlap integral $J^{F}=1.1\times10^{-13}\,cm^{3}\,M^{-1}$ is calculated for dyad **C2-PI** and a $J^{F}=1.3\times10^{-13}\,cm^{3}\,M^{-1}$ is derived for **C3-PI** and **C3-PPI**. A rate of energy transfer $k_{en}^{F}=5.0\times10^{11}\,s^{-1}$, $5.8\times10^{11}\,s^{-1}$, and $9.9\times10^{10}\,s^{-1}$ calculated for the dyads **C2-PI**, **C3-PI**, and **C3-PPI**, respectively. These rates are in agreement with the experimental results.

[37] a) H. S. Cho, D. H. Jeong, M. C. Yoon, Y. H. Kim, Y. R. Kim, D. Kim, S. C. Jeoung, S. K. Kim, N. Aratani, H. Shinmori, A. Osuka, *J. Phys. Chem. A* **2001**, *105*, 4200–4210; b) S. I. Yang, J. Seth, T. Balasubramanian, D. Kim, J. S. Lindsey, D. Holten, D. F. Bocian, *J. Am. Chem. Soc.* **1999**, *121*, 4008–4018; c) K. Pettersson, A. Kyrychenko, E. Ronnow, T. Ljungdahl, J. Martensson, B. Albinsson, *J. Phys. Chem. A* **2006**, *110*, 310–318.

[38] a) M. P. Eng, B. Albinsson, *Angew. Chem.* **2006**, *118*, 5754–5757; *Angew. Chem. Int. Ed.* **2006**, *45*, 5626–5629; b) J. Wiberg, L. J. Guo, K. Pettersson, D. Nilsson, T. Ljungdahl, J. Martensson, B. Albinsson, *J. Am. Chem. Soc.* **2007**, *129*, 155–163.

[39] A. Helms, D. Heiler, G. McLendon, *J. Am. Chem. Soc.* **1992**, *114*, 6227–6238.

[40] R. A. Marcus, *Angew. Chem.* **1993**, *105*, 1161–1172; *Angew. Chem. Int. Ed. Engl.* **1993**, *32*, 1111–1121.

[41] D. S. Pedersen, C. Rosenbohm, *Synthesis* **2001**, 2431–2434.

[42] M. W. Holman, R. Liu, D. M. Adams, *J. Am. Chem. Soc.* **2003**, *125*, 12649–12654.

[43] a) C.-H. Lee, J. S. Lindsey, *Tetrahedron* **1994**, *50*, 11427–11440; b) J. K. Laha, S. Dhanalekshmi, M. Taniguchi, A. Ambroise, J. S. Lindsey, *Org. Process Res. Dev.* **2003**, *7*, 799–812.

[44] R. Kumar, A. K. Chakraborti, *Tetrahedron Lett.* **2005**, *46*, 8319–8323.

[45] H. Langhals, J. Karolin, L. B.-Å. Johansson, *J. Chem. Soc. Faraday Trans.* **1998**, *94*, 2919–2922.

[46] P. G. Seybold, M. Gouterman, *J. Mol. Spectrosc.* **1969**, *31*, 1–13.

[47] L. Flamigni, *J. Phys. Chem.* **1993**, *97*, 9566–9571.

[48] L. Flamigni, N. Armaroli, F. Barigelletti, V. Balzani, J.-P. Collin, J.-O. Dalbavie, V. Heitz, J.-P. Sauvage, *J. Phys. Chem. B* **1997**, *101*, 5936–5943.

[49] a) L. Flamigni, *J. Phys Chem.* **1992**, *96*, 3331–3337; b) L. Flamigni, *J. Chem. Soc. Faraday I*, **1994**, *90*, 2331–2336.

[50] CS Chem3D Ultra CambridgeSoft. Com, Cambridge MA, USA, **2000**.

[51] Matlab 5.2., The MathWorks Inc., Natik, MA 01760, USA, **1998**.

Received: June 6, 2007
Published online: October 9, 2007

